Single cell transcriptomics identifies adipose tissue CD271^{+} progenitors for enhanced angiogenesis in limb ischemia

Oto Inoue,[1,5] Chiaki Goten,[1] Daiki Hashimuko,[1] Kosei Yamaguchi,[1] Yusuke Takeda,[1] Ayano Nomura,[1] Hiroshi Ootsuji,[1] Shinichiro Takashima,[1] Kenji Iino,[2] Hirofumi Takemura,[2] Manasi Halurkar,[5] Hee-Woong Lim,[3,4] Vivian Hwa,[4,5] Joan Sanchez-Gurmaches,[4,5,6,*] Soichiro Usui,[1,*] Masayuki Takamura[1,7,*]

Affiliations:

[1]Department of Cardiovascular Medicine, Graduate School of Medical Sciences, Kanazawa University, Kanazawa, Japan

[2]Department of Thoracic, Cardiovascular and General Surgery, Graduate School of Medical Sciences, Kanazawa University, Kanazawa, Japan

[3]Division of Biomedical Informatics, Cincinnati Children's Hospital Medical Center, Cincinnati, Ohio, USA

[4]Department of Pediatrics, University of Cincinnati College of Medicine, Cincinnati, Ohio, USA

[5]Division of Endocrinology, Cincinnati Children's Hospital Medical Center, Cincinnati, Ohio, USA

[6]Division of Developmental Biology, Cincinnati Children's Hospital Medical Center, Cincinnati, Ohio, USA

[7]Lead contact

[*]**Correspondences: juan.sanchezgurmaches@cchmc.org (J.S.G.), usuiso@staff.kanazawa-u.ac.jp (S.U.), mtakamura@staff.kanazawa-u.ac.jp (M.T.)**

HIGHLIGHTS

- Adipose tissue stromal cells have a distinct angiogenic gene profile among human cell sources.
- CD271^{+} progenitors in adipose tissue have a prominent angiogenic gene profile.
- CD271^{+} progenitors show superior therapeutic capacities for limb ischemia.
- CD271^{+} progenitors are reduced and functionally impaired in insulin resistant donors.

GRAPHICAL ABSTRACT

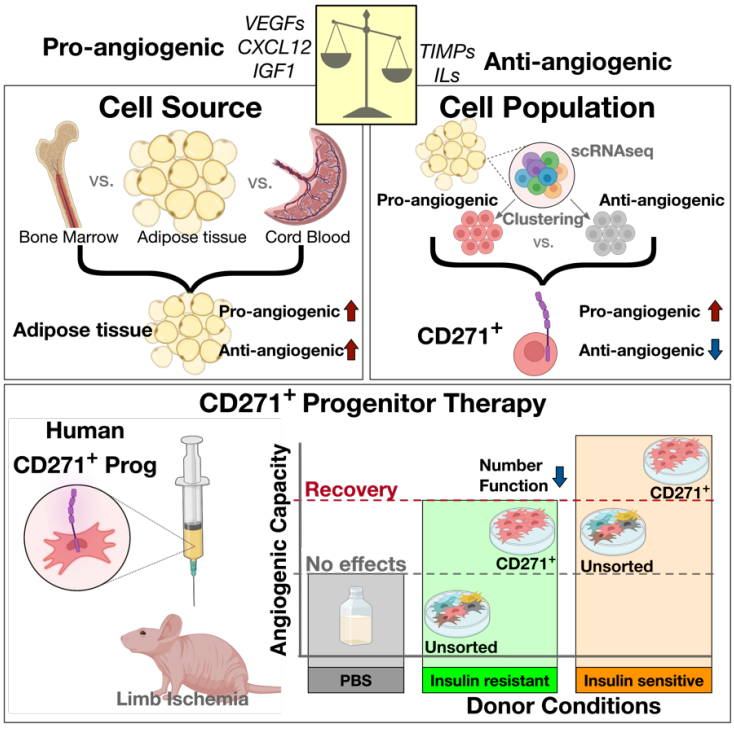

SUMMARY:

Therapeutic angiogenesis using mesenchymal stem/stromal cell grafts have shown modest and controversial effects in preventing amputation for patients with critical limb ischemia. Through single-cell transcriptomic analysis of human tissues, we identified CD271^{+} progenitors specifically from subcutaneous adipose tissue (AT) as having the most prominent pro-angiogenic gene profile distinct from other stem cell populations. AT-CD271^{+} progenitors demonstrated robust *in vivo* angiogenic capacity, over conventional adipose stromal cell grafts, characterized by long-term engraftment, augmented tissue regeneration, and significant recovery of blood flow in a xenograft model of limb ischemia. Mechanistically, the angiogenic capacity of CD271^{+} progenitors is dependent on functional CD271 and mTOR signaling. Notably, the number and angiogenic capacity of CD271^{+} progenitors was strikingly reduced in insulin resistant donors. Our study highlights the identification of AT- CD271^{+} progenitors with *in vivo* superior efficacy for limb ischemia. Furthermore, we showcase comprehensive single-cell transcriptomics strategies for identification of suitable grafts for cell therapy.

Keywords: single cell transcriptomics, therapeutic angiogenesis, cell therapy, CD271, adipose tissue, insulin resistance, peripheral artery disease, critical limb ischemia

INTRODUCTION

Critical limb ischemia (CLI), the end-stage of peripheral artery disease, is increasingly prevalent, in part due to the worldwide increase in obesity and diabetes.[1] Prognosis for patients with CLI is poor, comparable to malignant diseases.[2] One of the fatal features of CLI is atherosclerotic calcification, a condition difficult to treat even with currently available revascularization techniques such as catheter interventions and bypass surgery.[1] Consequently, at least 1 in 3 CLI patients are not eligible for revascularization therapies.[3] To combat this, the strategy of inducing neovascularization in ischemic tissues, known as therapeutic angiogenesis, has emerged as an attractive alternative therapy for CLI.[4]

Mesenchymal stem/stromal cells with regenerative capacities were discovered from multiple human organs including "harvestable" tissues such as bone marrow (BM), subcutaneous adipose tissue (AT), and umbilical cord blood (UCB).[5] The main reported therapeutic mechanism associated with cell therapy-induced neovascularization is through secretion of growth factors (i.e., VEGF, HGF, SDF-1) and extracellular vesicles from injected cells. [6,7] Preclinical studies of cell-based therapeutic angiogenesis using these cell sources showed favorable effects in animal models,[7-11] but have translated poorly in clinical trials. [4,7] For CLI, unsorted BM mononuclear cells are the most intensively evaluated in clinical trials. In a meta-analysis including 19 randomized controlled trials, cell therapy showed favorable effects on surrogate endpoints such

as pain score, pain-free walking distance, and ankle brachial index, but showed no significant benefits on primary endpoints including amputation-free rate and complete ulcer healing[12]. Prospective isolation of specific cell populations from BM mononuclear cells, based on $CD133^+$ or $CD34^+$ cells which were reported to be angiogenic preclinically,[10,13] also showed no evidence for lowering the risk of limb amputation in clinical trials.[14-16] Thus, a suitable cell population(s) optimal for therapeutic angiogenesis to achieve limb salvation has yet to be identified.

Single-cell transcriptomic technologies has revolutionized the capacity to identify lineages in tissue homeostasis and markers of specific stem cell populations.[17-20] However, application of single-cell transcriptomic analysis in cell therapy has been limited to only chimera antigen receptor T (CAR-T) cell therapy for lymphoma, where important cell populations for treatment response were assessed by single-cell RNA-sequencing (scRNA-seq). [21,22]

In this study, we took advantages of available scRNA-seq datasets generated from different human tissues to screen for cell surface markers that allow the segregation of a highly angiogenic subpopulation of cells. We identified that the $CD271^+$ cells specifically from AT have a distinct angiogenic gene profile with promising *in vivo* angiogenic capacity. Mechanistically, CD271/mTOR axis showed an important role for *in vivo* angiogenic capacity. Furthermore, we extend our findings to evaluate the feasibility and revascularization efficacy of $CD271^+$ cells from donors with cardiovascular disease (CVD). We obtained a sufficient number

of CD271^{+} progenitors from metabolically healthy CVD donors, and discovered superior therapeutic potentials over conventional cell grafts for patients suffering from CLI.

RESULTS

Adipose Tissue Lineage-negative Cells Show a Distinct Angiogenic Gene Profile among Human Stem Cell Sources

There is a strong need to identify the most suitable cell source for therapeutic angiogenesis. To search for subpopulations with pro-angiogenic capacity, we explored single cell gene expression profiles from readily available human stem cell sources. We analyzed available scRNA-seq datasets from bone marrow (BM),[23] umbilical cord-blood (UCB),[24] and stromal vascular fraction (SVF) of subcutaneous adipose tissue (AT)[25] from healthy donors (***n*** = 2/tissue, **Figure 1A** and **Table S1**). We performed dimension reduction with t-distributed stochastic neighbor embedding (tSNE) and cell clustering of a total of 47,035 cells (**Figure 1A-B and Figure S1**). To annotate clusters, marker genes for each cluster were collated manually based on reported markers in the Human Cell Atlas and the Human Protein Atlas (proteinatlas.org, **Figure S1**). [19,26,27] We removed mature immune and endothelial cells, i.e. Lineage-positive (Lin^+) cells,[26] from further analysis to enrich stem/progenitor cell populations. Since classic lineage markers of immune and endothelial cells differ between tissues, and $CD31^+$ cells are reported to be angiogenic only in BM[11], we used a well-established but distinct set of lineage-markers in each of these tissues[28-30] (listed in **Figure 1A**). Overall, we processed 18,053 Lin^- cells (BM; 9,289, UCB; 1,932, and AT; 6,832 cells, **Figure 1B**).

The main mechanism of cell-based therapeutic angiogenesis has been reported to be paracrine activities of soluble growth factors released by injected cells [6,31]. Thus, to further characterize angiogenic gene profiles of stem cell sources, we used a gene set of reported pro/anti-angiogenic factors released from tissue stem cells[6]. We updated the list with an additional gene set of 38 well-known secreted pro-/anti-angiogenic factors [32-34] (**Table S2**). Hierarchical clustering of BM, UCB, and AT Lin^- cells based on expression of pro-/anti-angiogenic factor genes clearly isolates AT cells as having a distinctive gene expression profile. This was characterized by prominent expression of pro-angiogenic factors including *MMP2*, *CXCL12*, *VEGFs* and *IGF1* (**Figure 1C**). Consistently, gene enrichment analysis resulted in a number of pro-angiogenic pathways which were significantly enriched in AT compared to BM or UCB (**Figure 1D**). On the other hand, we observed that anti-angiogenic factors such as *TIMP2* and *TIMP3* were also upregulated in AT (**Figure 1C**). Therefore, we hypothesized that AT would be an attractive cell source if pro-angiogenic cells could be segregated from TIMP2/3 expressing anti-angiogenic cells.

Adipose Tissue scRNA-seq Analysis Filtered 30 Surface Markers of Angiogenic Cells

To delineate angiogenic populations within the AT, we analyzed Lin^-CD34^+ progenitors on available scRNA-seq datasets from six non-diabetic human subcutaneous AT SVF (**Figure 2A**). Louvain clustering divided AT Lin^-CD34^+ progenitor cells[8,35] into 3 progenitor groups (**Figure**

2B and Figure S2A). To understand the nature of each of these clusters, we analyzed the top 10 marker genes of each Progenitor cluster (**Figure 2C**). Progenitor 1 cluster was characterized by higher expression of adipocyte lineage markers (*APOE,* and *CEBPD*), while Progenitor 2 by mesenchymal/fibrotic markers (*FBN1*, *MFAP5*, and *FN1*). Progenitor 3 highly expressed some adipocyte lineage markers common to Progenitor 1, including *APOD*, but was characterized by higher expression of non-adipocyte markers *MYOC* and *IGFBP3*. Among these 3 clusters, pathway enrichment analysis found that Progenitors 1 & 3 were dominated by genes involved in sprouting angiogenesis and lipogenesis (**Figure 2D**). Based on this analysis, Progenitors 1 & 3 were defined as pro-angiogenic clusters while Progenitor 2 was defined as an anti-angiogenic cluster. Using the same gene set as for cell source screening (**Figure 1C** and **Table S1**), we compared pro/anti-angiogenic factor genes between the pro- and anti-angiogenic clusters. The expression level of pro/anti-angiogenic factors clearly separates pro- and anti-angiogenic clusters on our reanalyzed scRNA-seq datasets from six non-diabetic human subcutaneous AT SVF (**Figure 2A, S2B**). Among the 38 genes in the gene set, 22 genes were differentially expressed between pro/anti-angiogenic clusters. As expected, the pro-angiogenic cluster showed higher expression of 12 pro-angiogenic factors, while all 5 anti-angiogenic factor genes were highly expressed in the anti-angiogenic cluster (**Figure S2B**).

To obtain intact cell populations for cell therapy purposes, purification procedures

utilizing surface markers are necessary. Thus, we next focused on identifying the surface markers specifically expressed in the pro-angiogenic cluster that would be suitable for downstream flow cytometric isolation. Based on 2,621 differentially expressed genes between pro-/anti-angiogenic clusters from scRNA-seq analysis identified when grouping data from the six samples analyzed (**Figure 2E**, **Figure S2C and Table S3**), a total of 30 surface protein-encoding genes (**Table S4**) were identified. We concluded that these 30 surface proteins may potentially lead to the specific isolation of pro-angiogenic cells.

Next, we determined which marker from the filtered 30 surface protein-encoding genes would be the most suitable for cell graft preparation for therapeutic angiogenesis. To achieve this, we evaluated the specificity of the 30 individual surface proteins enriched in the pro-angiogenic cluster by analyzing the number of cells that express each protein in each cluster using the data from the same six non-diabetic human subcutaneous AT SVF (**Figure 2A, 2F**). From this analysis, 5 surface markers were identified for isolating pro-angiogenic cells with over 95% purity (**Figure 2G**). Among them, CD271 (Low-affinitive nerve growth factor receptor, LNGFR) emerged as the top-ranked surface marker, closely followed by VCAM1 (vascular cell adhesion molecule 1) and ABCB11 (ATP binding cassette subfamily B member 11). In particular, from the cells detected to express CD271, 98% were on the pro-angiogenic cluster (**Figure 2G**). This is appreciably higher compared to $Lin^{-}CD34^{+}$ progenitors (Prog 1,2, and 3) and to other

previously known AT progenitor markers[36] such as CD105, CD90, and CD73 (**Figure 2G**). Furthermore, out of the cells labelled by CD271 expression less than 3% were on the anti-angiogenic cluster, which was the lowest contamination rate amongst all studied markers (**Figure 2G**). Thus, we identified surface markers that may efficiently select for pro-angiogenic cells.

Adipose Tissue CD271$^+$ Cells are Highly Angiogenic

Next, we further analyzed the top three surface markers identified in our analysis aiming to find which cell population showed the highest angiogenic potential. We noted that CD271$^+$, VCAM1$^+$, and ABCB11$^+$ cell subpopulations are distinct, with very few cells carrying all three markers, or even 2 of the 3 markers (**Figure 3A**). In particular, over 80% of CD271$^+$ cells were VCAM$^-$/ABCB11$^-$. Therefore, we performed pathway enrichment analysis for subpopulations carrying each single marker, i.e. comparing between CD271$^+$VCAM$^-$ABCB11$^-$, CD271$^-$VCAM$^+$ABCB11$^-$, and CD271$^-$VCAM$^-$ABCB11$^+$. Strikingly, CD271$^+$ cells showed pro-angiogenic pathway enrichment over VCAM1$^+$ or ABCB11$^+$ cell populations (**Figure 3B**). Direct comparison between CD271$^+$ and CD271$^-$ populations showed that CD271$^+$ cells have higher expression of important pro-angiogenic factors (e.g., *MCP1*, *CXCL12*, *CTGF*, and VEGFA **Figure 3C**). Additionally, anti-angiogenic factors *TIMP2* and *TIMP3* were downregulated in CD271$^+$ cells compared to CD271$^-$ cells (**Figure 3C**).

We next asked if it is possible to obtain sufficient number of CD271$^+$ cells from AT for

therapeutic angiogenesis. We found that the number of CD271 expressing cells were at least 10 times higher in AT than in BM or UCB (**Figure 3D**). To confirm these results, we performed flow analysis on SVF cells of human subcutaneous AT. Consistently, we detected CD271 protein in at least 5–10% of total SVF cells of human subcutaneous AT (**Figure 3G**); in contrast, it was previously reported that less than 0.1% of individual BM cells expressed CD271 protein by flow analysis.[37] From these data, we concluded that AT is the most suitable tissue for harvesting sufficient number of $CD271^+$ cells.

Although AT carried higher numbers of $CD271^+$ cells than either BM or UCB, we assessed whether $CD271^+$ cells are pro-angiogenic, independent of tissue source. As expected, AT-$CD271^+$ cells showed strong enrichment in proangiogenic pathways when compared to AT-$CD271^-$ cells (**Figure 3E**). BM-$CD271^+$ cells, in contrast, were characterized by pathways related to the cell cycle and proliferation (**Figure 3E**), consistent with a previous report that BM-$CD271^+$ cells possess clonogenic and multi-lineage differentiation capacities.[37] On the other hand, UCB-$CD271^+$ cells showed upregulation of immune system-related pathways when compared to UBC-$CD271^-$ (**Figure 3E**). These transcriptomic analyses indicated that although $CD271^+$ cells are available from different tissues, AT-$CD271^+$ cells exhibit a distinct, pro-angiogenic, gene profile.

It is of note that several subpopulations of BM, including $CD34^+$ [14], $CD133^+$ [16], and

CD31^{+} [11] populations, have been reported to be angiogenic and also have been tested in clinical trials. Thus, we compared transcriptomic profile of AT-CD271^{+} cells to these three BM subpopulations (**Figure 3F**). We found that AT-CD271^{+} cells consistently showed enrichment of pathways related to cell differentiation while BM subpopulations were characterized by involvement with immune systems. More importantly, AT-CD271^{+} cells demonstrated enrichment of pro-angiogenic pathways (e.g. activating endothelial proliferation and VEGF signaling) when compared to each BM subpopulation. Altogether, these transcriptomic data indicate that AT-CD271^{+} cells has higher angiogenic potential than candidates already in clinical trials.

AT-CD271^{+} progenitors are culture-expandable with classical mesenchymal stem cell capacity

It is known that culture-expandable mesenchymal stem cell-like cells can be generated from unsorted AT-progenitors, and are commonly referred as adipose-derived stem cells (ADSCs) [38]. To better understand human AT-CD271^{+} cell biology, we sorted and established *in vitro* cultures of CD271^{+} and CD271^{-} cells from subcutaneous AT of human healthy subjects (**Figure 3G**). Both types of cells were adherent and proliferative with similar spindle-shaped morphology (**Figure 3H**). CD271^{+} cells, however, showed enhanced proliferative capacity compared to CD271^{-} cells as determined by colony formation assay where CD271^{+} cells generated larger and more dense colonies (**Figure 3H**) in significantly higher number (**Figure**

3I). Both cell types readily differentiated into adipocyte (Oil Red O) and osteoblast (Alizarin Red) lineages (**Figure 3J**). Collectively, these *in vitro* assays characterized CD271$^+$ progenitors as culture-expandable with classical ADSC morphology and capacities.[38]

CD271$^+$Progenitors Demonstrate Enhanced In Vivo Angiogenic Capacity with Long-Term Engraftment

We next examined the *in vivo* angiogenic capacity of CD271$^+$ progenitors in a xenograft model of limb ischemia (**Figure 4A**). For this, we injected PKH-labeled human CD271$^+$ or CD271$^-$ progenitors (0.5 million cells / mice) directly into limb muscles of immunocompromised mice that are subjected to left femoral artery ligation. Cell-treated limbs were harvested at day 7, 14, and 35 after fluorescence-conjugated isolectin perfusion to detect capillaries with blood flow [9,29,39].

In this xenograft model, we observed that CD271$^+$ progenitors clearly engrafted better than CD271$^-$ progenitors in ischemic limb, with 2-3 times higher PKH$^+$ cell numbers (**Figure 4B-C**). The enhanced differences in engraftment capacity of AT-CD271$^+$ progenitors persisted for up to 5 weeks. Further, immunofluorescent analysis of tissue sections shows that AT-CD271$^+$ progenitors localize around lectin$^+$ capillaries (**Figure S3A**). To clarify whether injected CD271$^+$ progenitors were potentially trans-differentiating to endothelial cells, we performed flow cytometric analysis of PKH$^+$ cells from digested limb muscles 14 days after cell engraftment

(**Figure S3B**). We confirmed that only 6% of engrafted CD271$^+$ progenitors expressed the endothelial marker CD31, which suggested the majority of the injected cells did not undergo differentiation into mature endothelial cells, at least not within the time frame of the protocol (**Figure S3C**). On the other hand, isolated PKH$^+$ cells maintained expression of human CD271 and typical markers of cultured ADSCs[36] (human CD90 and CD105) (**Figure S3C**). These findings confirmed that engrafted CD271$^+$ progenitors preserve their stem cell marker expressions and likely acted as stem/progenitor cells to support intrinsic regeneration.

Correlating with higher survival of engraftment, CD271$^+$ progenitor therapy induced enhanced revascularization after limb ischemia. This is evidenced by 3-fold higher capillary density (Lectin$^+$ and mouse CD31$^+$, **Figure S3D**) than that induced by CD271$^-$ progenitors (**Figure 4D**). Strikingly, CD271$^+$ progenitors successfully led to recovery of blood flow in treated limb, to a level comparable to healthy limbs, as determined by both imaging and doppler blood flow analysis (**Figure 4E-F**).

To confirm tissue reparative capacity of CD271$^+$ progenitors, we incorporated *in vivo* EdU labeling into our *in vivo* protocol (**Figure 4G**). Since neovascularization and blood flow recovery were favorably accomplished by day 14 in our model, we evaluated EdU incorporation on day 7 when tissue neovascularization was in progress. *In vivo* EdU labeling demonstrated that treatment with CD271$^+$ progenitors led to approximately four times higher proliferation of host

cells (largely composed of skeletal muscle cells and endothelial cells and identified as PKH$^-$) than treatment with CD271$^-$ progenitors (**Figure 4H-I**). Collectively, the data from our xenograft model provide promising translational *in vivo* angiogenic capacity of CD271$^+$ progenitors with long-term engraftment and enhanced host cell proliferation.

Mutant CD271 Impairs the Angiogenic Gene Profile and Therapeutic Capacity of mouse ADSCs

We next explored potential mechanisms that drove angiogenic capacity of CD271$^+$ progenitors. Reanalysis of scRNA-seq datasets of SVF cells from neonatal mice inguinal fat pads[40] subclustered cells into 10 clusters (**Figure 5A and Figure S4A-B**). CD271$^+$ progenitors were distributed predominantly with Schwann cell, pericytes, and Lin$^-$ Progenitor clusters (**Figure S4B**). Consistent with human CD271$^+$ progenitors gene expression profiles (**Figure 3C**), mouse CD271$^+$ showed upregulation of pro-angiogenic factors including *Igf1* and *Cxcl12*, and downregulation of anti-angiogenic factors *Timp2* and *Timp3*. (**Figure 5B**). Furthermore, mouse AT-CD271$^+$ progenitors showed enrichment of angiogenesis-related GO terms (endothelial cell proliferation and VEGF signaling pathway, **Figure 5C**). We asked whether a functional CD271 protein is necessary for the angiogenic capacity of CD271$^+$ progenitors in mice. We used mice lacking exon 3 of the CD271 gene which encodes three of the four necessary cysteine-rich repeats in the extracellular domain. The loss of exon 3 generated an in-frame mutant CD271

protein with a 2- to 3-fold reduction in ligand binding[41] (**Figure 5D**). We established cultured mouse ADSCs from wild-type littermates (Control) and CD271 mutant mice ($CD271^{Mut}$). Compared to Control-ADSCs, $CD271^{Mut}$ ADSC transplants demonstrated impaired cell engraftment (**Figure 5E-F**), impaired *in vivo* angiogenesis (**Figure 5G**), and reduced blood flow recovery (**Figure 5H-I)**. This data suggests that normal CD271 activity is required for $CD271^{+}$ cells to have full angiogenic capacity. This highlights an important new biological function of CD271 and proposes the concept that CD271 is not only a surface marker for cell selection.

We asked what downstream signaling pathways of CD271 may participate in the angiogenic functions of $CD271^{+}$ progenitors. CD271 can induce cell death or cell survival, depending on interacting coreceptors.[42] Among the three known coreceptors of CD271, tropomyosin receptor kinase B (TRKB), which coordinates with the mTOR pathway for cell survival[43] (**Figure S5A**), was predominantly expressed in human AT-$CD271^{+}$ progenitors while cell expressing the other coreceptors were rarely found (**Figure S5B**). We confirmed that over 95% of $CD271^{+}$ progenitors co-expressed TRKB protein even under cultured condition (**Figure S5C**). Cultured $CD271^{+}$ progenitors also showed higher expression of *MTOR* than $CD271^{-}$ progenitors (**Figure S5D**). Furthermore, the known downstream genes regulated by mTOR signaling, i.e., *HIF1A* and *VEGFA*, were significantly upregulated in $CD271^{+}$ progenitors compared to $CD271^{-}$ (**Figure S5D**). Consistent with previous reports of positive feedback

between mTOR and SDF-1 (CXCL12)[44], *CXCL12* was also highly expressed in CD271^{+} progenitors (**Figure S5D**). Interestingly, we noted that in mouse CD271^{Mut} ADSCs, *Mtor* expression was reduced by ~50% (**Figure S5E**), which resulted in concomitant inhibition of downstream factors *Hif1a*, *Vegfa*, and *Cxcl12* (**Figure S5E**). From these observations, we hypothesized that the downstream mTOR pathway activated by CD271 may be required for the angiogenic capacity of CD271^{+} progenitors. To test this hypothesis, we knockdown mTOR in human ADSCs (cultured unsorted AT cells) using short interfering RNAs (si-mTOR ADSCs). Gene expression analysis showed efficient knockdown of mTOR (**Figure S5F**). Additionally, si-mTOR ADSCs shown downregulated expression of *VEGFA* and *CXCL12* (**Figure S5F**). Next, we functionally tested the effects of decreased mTOR levels in cell therapy experiments using our ischemic limb mouse model. si-mTOR treatment resulted in loss of *in vivo* angiogenic capacity of ADSCs as evaluated by capillary density (**Figure S5G-H**), engraftment (**Figure S5I**) and tissue reparative capacity evaluated by the number of proliferating cells (**Figure S5J-K**). Together, our findings strongly suggest that a functional CD271/mTOR axis is necessary for full ADSC angiogenic capacities.

CD271^{+} Progenitors from Insulin Resistant Patients are Decreased and Have Poor Therapeutic Potential

Next, we asked if AT-CD271^{+} progenitors are available in sufficient number to be used in clinical

settings. For this, we analyzed patient-derived AT samples. First, we evaluated the number of $CD271^+$ progenitors in subcutaneous AT from 38 CVD patients with various pathological conditions and diseases (**Table S4).** The frequency of $CD271^+$ progenitors in SVF cells ($CD271^+$/SVF) ranged from 0.2 to 40% and was not significantly affected by donor sex, BMI, or age (**Figure 6A**). This is clearly favorable for cell preparation from a variety of donors. Intriguingly, the number of $CD271^+$ progenitors was negatively correlated with the insulin resistance score (HOMA-IR) (**Figure 6A**). Consistently, $CD271^+$ progenitor number was reduced by approximately 75% in patients with insulin resistance (HOMA-IR > 2.9)[45] as determined by flow cytometry (**Figure 6B**). Because immune cells accumulate in insulin-resistant AT, we additionally calculated the percentage of $CD271^+$ progenitors in Lin^-CD34^+ cells. Consistently, $CD271^+/Lin^-CD34^+$ SVF was also significantly reduced in patients with insulin resistance (**Figure 6B**). To validate the finding of our 38 CVD patient cohort with an orthogonal method, we analyzed available subcutaneous AT scRNA-seq datasets from lean healthy (insulin sensitive) subjects versus obese type 2 diabetic (insulin resistant) subjects (**Figure 6C and Figure S6A**). We found a significant reduction in the number of $CD271^-$ expressing cells in AT from insulin resistant subjects (**Figure 6D-E**). Furthermore, GO enrichment analysis shows decreased angiogenesis-related terms in $CD271^+$ progenitors from insulin resistant donors when compared to $CD271^+$ progenitors from insulin sensitive donors (**Figure 6F and Table S5**).

Since our results show that CD271$^+$ progenitors have a positive therapeutic effect in our mouse ischemic limb model, we next hypothesized that CD271$^+$ progenitor therapy is more beneficial over conventional unsorted ADSCs in our model. Hence, we prepared paired unsorted ADSCs and sorted CD271$^+$ progenitors from 5 insulin resistant and 5 insulin sensitive patient subgroups from our 38-patient cohort (**Figure 6A-B**) to test their therapeutic effectiveness in our ischemic limb mice model (**Figure 6G**). As shown in **Figure 6H**, sorted human CD271$^+$ progenitors showed markedly enhanced engraftment over conventional ADSCs from the same donors. Notably, cell therapy with CD271$^+$ progenitors of metabolically healthy donors resulted in improved engraftment than CD271$^+$ progenitors of insulin resistant donors (**Figure 6H**). Interestingly, although CD271$^+$ progenitors from both insulin resistant and metabolically healthy donors increased capillary density compared to respective unsorted cells, CD271$^+$ progenitors of metabolically healthy donors achieved striking higher capillary density than those from insulin resistant donors (**Figure 6I**). It is important to note that conventional unsorted ADSCs from insulin resistant donors showed capillary density equivalent to PBS injection suggesting very limited effect of this population (**Figure 6I**). Finally, CD271$^+$ progenitors from insulin sensitive donors achieved full recovery of blood flow (**Figure 6J**) while CD271$^+$ progenitors from insulin resistant donors were less effective but still achieved a remarkable > 85% recovery. These data further highlight the promising efficacy of CD271$^+$ progenitor therapy for ischemic limb, even

from insulin resistant donors, albeit therapy from insulin sensitive donors may lead to better long-term outcomes as engraftment is higher and improve the angiogenic capacity of the ischemic lesion.

Preliminary Positive Impacts of Autologous CD271$^+$ Progenitors in a Trial Outcome of SVF Therapy for CLI

To further investigate the therapeutic potential of CD271$^+$ progenitors, we retrospectively evaluated data from a limited human cell therapy trial (multi-center clinical trial of SVF therapy) for no-option CLI patients[46] (**Figure 7A** and **7B**). During the one-year follow-up period, patients received no interventional treatments (e.g. catheter intervention, surgery). Medications were already optimized prior to SVF therapy under consensus guidelines, and no further changes were made [47]. Of the 4 patients within our trial who underwent SVF therapy (**Table S6**), 2 patients exhibited complete recovery (disappearance of ulcer lesion, **Figure S7**) and 2 cases resulted in either major amputation or ulcer recurrence at the 1-year follow-up post-SVF therapy (**Figure 7B** and **7D**). All 4 patients had HOMA-IR within normal range (min-max 0.3-2.0, mean 1.4, **Table S7**). Based on the above results, we hypothesized that successful recovery at the 1-year follow up is correlated to the number of CD271$^+$ progenitors initially injected. Thus, we retrospectively evaluated the potential impact of injected CD271$^+$ progenitor number on efficacy of SVF therapy (**Figure 7C**). Then, we stratified patients based on recurrence or amputation outcome and

revisited the composition of cell initially injected. Although patient number in this analysis is very small, we observed that our primary outcome does not correlate with total SVF nor with the $Lin^{-}CD34^{+}$ cell number injected (**Figure 7E**). In particular, patient 2 who required amputation, had received the highest dose of total SVF cells and $CD34^{+}$ cells compared to those of the patients who recovered, suggesting that high doses of $CD34^{+}$ cells was insufficient for preventing amputation. However, both patients that completely recovered from ulcers without recurrence (patient 1 and 4) were injected with higher number of $CD271^{+}$ cells (**Figure 7E**). As an example, Patient 1, who recovered from CLI, had approximately 200 times higher number of $CD271^{+}$ progenitors injected than patient 3 who presented with recurrent ulceration (**Figure 7C** and **F**). The positive correlation between full recovery and $CD271^{+}$ progenitors injected was striking especially when we compared the number of injected $CD271^{+}$ progenitors per ulcer area (***n*** = 6 ulcer lesions, **Figure 7F**). Collectively, our findings from this sub-analysis of SVF therapy for CLI, strongly support the significance and positive therapeutic effects of $CD271^{+}$ progenitors.

DISCUSSION

Despite decades of research in therapeutic angiogenesis, the ideal cell population for grafting remains to be fully determined. This is evidenced by controversial effects on amputation prevention in 19 RCTs (837 patients) using 5 cell types[12]. In this study, we used unbiased single-cell transcriptomics to identify adipose tissue CD271^{+} progenitors as a human pro-angiogenic cell population with the strongest potential for efficacious therapeutics. Traditionally, the identification of cell populations suitable for cell therapy had depended on biased selection of markers, from which appropriate marker-positive cell populations were isolated for in-depth analysis *in vitro* and *in vivo*. This potential hit-and-miss strategy is time consuming and costly, and allow the analysis of only a limited number of markers.[48] In this study, we took advantage of current single cell genomic approaches to simultaneously explore all known/detected surface markers. Based to these unbiased analyses of available scRNA-seq datasets, we found that AT-CD271^{+} progenitors were predominantly pro-angiogenic with less than 3% of antiangiogenic cells. We suggest that application of single-cell transcriptomics for cell therapy can greatly improve discovery of better cell markers for targeted therapies of interest. Furthermore, we took advantage of evaluating cell populations with opposing functions through scRNAseq analysis, i.e. therapeutic (pro-angiogenic) and harmful (anti-angiogenic) populations. Although an extra purification step to exclude anti-angiogenic cells was not necessary due to the extremely low rate

of anti-angiogenic cells in CD271^{+} progenitors, sorting methodologies to isolate therapeutic marker-positive away from harmful marker-negative cells could be strategic. For example, immune-modulatory cell therapy for graft-versus-host disease,[49,50] which is increasingly evaluated in clinical trials but with inconsistent outcomes, might benefit from such a strategy to avoid pro-inflammatory cell engraftment.

The relationship between CD271 expression and cell angiogenic capacity has been poorly established. There is a report demonstrating that CD271^{+} progenitors secreted angiogenic factors *in vitro*.[51] However, limited angiogenesis was concomitantly observed in a mouse model of CD271^{+} cell injection for cartilage repair.[52] Based on our present results, CD271^{+} progenitors could exhibit angiogenic capacity specifically in ischemic-type diseases. Interestingly, previous demonstrations that CD271^{+} cell/HUVEC coculture, but not conditioned medium, could enhance the tube formation of HUVECs, suggest the importance of cell-to-cell interactions between CD271^{+} progenitors and target cells. [51,52] In our xenograft model, we observed CD271^{+} progenitors were surrounding capillaries and labeled by perfused lectin as with capillaries (**Figure 4B-C** and **Figure S3A**). This indicates the close proximities between "leaky" capillaries and engrafted cell grafts. Taken together, we conclude engraftment capability and cell-cell interactions between cell grafts and the regenerating (immature) capillaries would be important for CD271^{+} progenitors to exert angiogenic functions.

CD271, also known as LNGFR, is a transmembrane receptor originally found to be a marker for neural lineage cells. CD271 is known to activate mTOR through cooperation with coreceptors including TRKB, also known as NTRK2 (neurotrophic receptor tyrosine kinase 2) [42,53] a coreceptor which we found to be abundantly expressed in the majority of CD271^{+} progenitors from human SVF cells. Data from single-cell transcriptomics, mutant CD271 mouse model, and mTOR silencing studies, all supported the participation of CD271/mTOR axis in the angiogenic capacity of CD271^{+} progenitors. However, our si-mTOR studies may reflect general blunted impacts since the mTOR pathway is a well-established major signaling hub for multiple factors. Our results, nevertheless, highlight the importance of mTOR activity for evaluating ADSC quality. Future studies should assess whether neurotrophic factors may enhance CD271/TRKB/mTOR signaling in CD271^{+} progenitors and if neurotrophin pretreatment or controlled CD271 overexpression might be preconditioning strategies for enhancing angiogenic effects of cell grafts.

In this study, we observed proliferative and angiogenic capacity of AT-CD271^{+} progenitors. We found that angiogenic AT-CD271^{+} progenitor populations were reduced in patients with insulin resistance, although the causal relationship between AT-CD271^{+} progenitor decrease and insulin resistant is unclear from our study. Since blunted mTOR signaling in AT can lead to insulin resistance,[43,54] the CD271/mTOR axis in AT may have protective roles against

insulin resistance. This may be important under obesogenic stimuli (e.g., overfeeding), when AT dramatically increases its size and appropriate angiogenesis is essential in obesity to prevent hypoxia which triggers AT inflammation and subsequently insulin resistance.[55-58] Future detailed investigations of the CD271/mTOR axis in AT will provide better understanding of insulin resistance pathophysiology and may reveal novel strategies to prevent metabolic syndrome.

Although preclinical studies suggested promising efficacy of cell therapy, clinical trials have shown inconsistent results. This might be explained by numerical or functional differences of cell grafts among CVD patients [59,60]. In this study, we demonstrated decreased cell number and functional impairment of $CD271^+$ progenitors in insulin resistant donors. Given the higher incidence of metabolic disorders in CVD patients, our findings have great implications for effective cell therapy in CVD. It is critical to overcome the reduction in cell number and the functional impairment of $CD271^+$ progenitors in insulin resistant donors if efficient $CD271^+$ cell therapy is to be developed. We and others have previously reported altered gene expression and impaired angiogenic effects of ADSCs derived from type 2 diabetic patients compared to ADSCs from nondiabetics.[61,62] In this study, we found that HOMA-IR can be used as a surrogate marker to predict quantity and quality of $CD271^+$ progenitors in AT. Therefore, HOMA-IR evaluations may mitigate ineffective therapeutic interventions by permitting screening of appropriate donors for therapeutic angiogenesis, not only for autologous therapy, but also for allograft (cell bank)

development.

Our single cell transcriptomics from multiple stem cell sources captured AT as a better cell source for angiogenic cell populations than current BM mononuclear cells. Furthermore, we showed $CD34^+$ selection did not increase the quantity of appropriate angiogenic cell population when compared to unsorted SVF (**Figure 2H**). Here, we propose that targeted CD271 selection is a novel strategy for preparing cell graft with $CD271^+$ progenitor therapy expected to improve cell therapeutic outcomes. Although $CD271^+$ progenitors showed more angiogenic gene profiles over the other candidate cell populations we screened (ABCB11 and VCAM1) or previously reported (BM-$CD34^+$, $CD133^+$, and $CD31^+$), we did not compare angiogenic capacity directly in this study. Further studies to compare $CD271^+$ progenitors and other potential subpopulations *in vitro* and *in vivo* would be important to develop the most suitable strategy for therapeutic angiogenesis. More importantly, as demonstrated in this study (**Figure 6** and **7**), the feasibility/accessibility of these cell populations in human donors should be tested to successfully translate our findings into clinical trials.

Our retrospective analysis of the SVF therapy trial for terminal CLI [46] supports a positive correlation between complete recovery and high numbers of injected $CD271^+$ progenitors, while amputated/recurrence of CLI was associated with low numbers. Importantly, we determined that approximately 300,000 to 500,000 AT-$CD271^+$ progenitors per lesion area

($CD271^+$ cells / ulcer cm^2) as the dose that seems to be necessary for favorable outcome. Fortunately, this is a dose which, in our experience, should be readily feasible to prepare from CVD patients. Future studies and clinical trials focusing on $CD271^+$ progenitor therapy in larger cohorts will provide the necessary clinical evidence for efficacy and dosing requirements.

In summary, we applied single-cell transcriptomics for cell therapy purposes against CLI and identified a human stem cell population which is readily available and possesses the most angiogenic gene profile. $CD271^+$ progenitors can be readily harvested from human subcutaneous AT and exhibit promising angiogenic capacities, including long-term engraftment and augmentation of host tissue cell proliferation in cell therapy. In CVD patients with systemic insulin resistance, the number and angiogenic capacity of $CD271^+$ progenitors were significantly decreased. $CD271^+$ progenitors obtained from insulin sensitive donors, in contrast, demonstrated the highest *in vivo* angiogenic capacity and consistently rescued ischemic limb. Our data highlight the potential screening benefits using single-cell technologies and evident benefits of $CD271^+$ progenitor transplantation for improving current therapeutic angiogenesis.

Study Limitations

In this study, the correlation between the expression levels of CD271 mRNA and protein was not directly analyzed. Although we confirmed higher mRNA expression of CD271 in sorted $CD271^+$ progenitors (data not shown), further studies using single-cell multiomics technologies, including CITE-seq,[63] would be helpful to validate our results.

In mouse ADSC experiments, we observed that a mutation of the CD271-encoding gene decreased angiogenic factor expression and impaired *in vivo* angiogenic capacity in unsorted mouse ADSCs. We did not sort $CD271^+$ cells from $CD271^{Mut}$ mice because of difficulties in detecting mutated CD271 with currently available monoclonal antibodies.

Finally, we could not definitely determine whether injected $CD271^+$ progenitors transdifferentiate into endothelial cells or not. Although expression of human CD31 was observed in only a small proportion of engrafted $CD271^+$ progenitors, the histological assessment demonstrated that they were morphologically similar to stromal or perivascular cells than to endothelial cells. Single-cell analysis of regenerating tissues after cell therapy might provide more detailed information about the transcriptomic dynamics of injected $CD271^+$ progenitors.

ACKNOWLEDGEMENTS

We would like to acknowledge the support and collaborations of Professor Toyoaki Murohara, Dr. Rei Shibata, Dr. Yuuki Shimizu, and TACT-ADRC multicenter trial Group regarding SVF therapy trial. Additionally, we appreciate Professor Yoh Takuwa and Dr. Kazuaki Yoshioka for the assistance in Laser Doppler analysis for blood flow quantification. Furthermore, we thank Dr. Jun Kinoshita, Dr. Katsunobu Oyama, Dr. Yukio Fushida, and the other operating staff of Kanazawa University Hospital for providing adipose tissue samples to this study. Finally, we appreciate the study participants and their families. Diagrams in Figures were created with BioRender.com.

FUNDING

This study has been supported by Japan Society for the Promotion of Science (JSPS) KAKENHI (Tokyo, Japan) Grant Number JP16H06828. OI is supported by Japanese Heart Foundation Research Abroad Award 2021. JSG is supported by grants from the American Heart Association (18CDA34080527), the NIH (R21OD031907), a CCHMC Trustee Award, a CCHMC Center for Pediatric Genomics Award and a CCHMC Center for Mendelian Genomics & Therapeutics Award. The content is solely the responsibility of the authors and does not necessarily represent the official views of the National Institutes of Health.

AUTHOR CONTRIBUTIONS

Conceptualization: O.I., V.H., J.S.G., S.U., M.T.

Methodology: O.I., C.G., D.H., K.Y., Y.T., A.N., H.M., J.S.G., S.U.

Validation: O.I., C.G., D.H., K.Y., Y.T., A.N., H.M., J.S.G., S.U.

Formal Analysis: O.I., A.N., D.H., K.Y., H.W.L., J.S.G., S.U.

Investigation: O.I., C.G., D.H., K.Y., Y.T., A.N., H.O., S.T., H.M., H.W.L., J.S.G., S.U.

Resources: K.I., H.T.

Data Curation: O.I., H.W.L., V.H., J.S.G., S.U.

Writing – Original Draft: O.I., C.G., V.H., J.S.G., S.U., M.T.

Writing – Review & Editing: O.I., C.G., D.H., K.Y., Y.T., A.N., H.O., S.T., K.I., H.T., H.M., H.W.L., V.H., J.S.G., S.U., M.T.

Visualization: O.I., H.W.L., V.H., J.S.G., S.U.

Supervision: J.S.G., S.U., M.T.

Project Administration: J.S.G., S.U., M.T.

Funding Acquisition: J.S.G., S.U., M.T.

COMPETING INTERESTS

The authors declare no competing interests.

INCLUSION ANS DIVERSITY

We worked to ensure gender balance in the recruitment of human subjects. We worked to ensure ethnic or other types of diversity in the recruitment of human subjects. One or more of the authors of this paper self-identifies as an underrepresented ethnic minority in their field of research or within their geographical location.

Figure 1

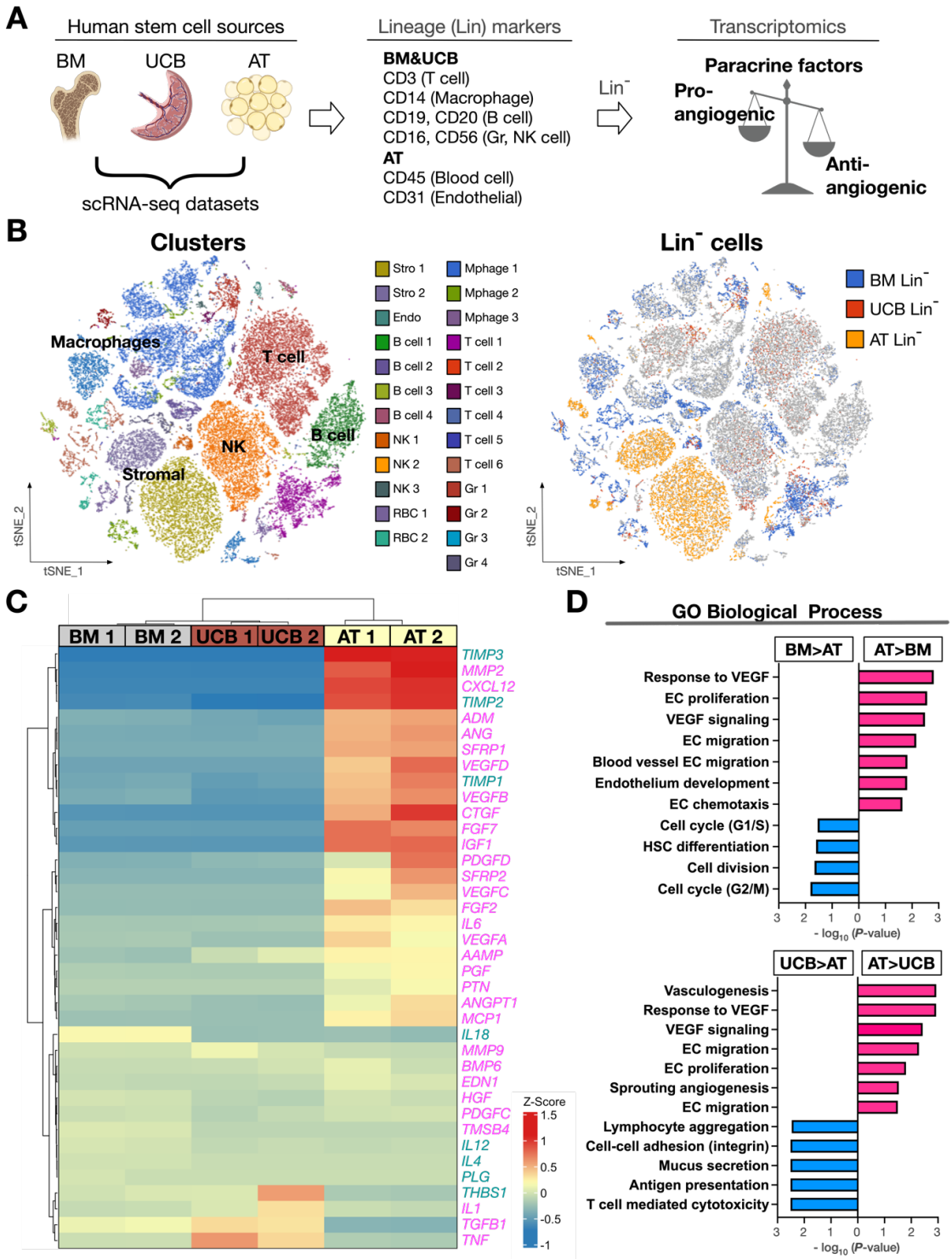
A
Human stem cell sources
BM
UCB
AT
scRNA-seq datasets
Lineage (Lin) markers
BM&UCB
CD3 (T cell)
CD14 (Macrophage)
CD19, CD20 (B cell)
CD16, CD56 (Gr, NK cell)
AT
CD45 (Blood cell)
CD31 (Endothelial)
Lin⁻
Transcriptomics
Paracrine factors
Pro-angiogenic
Anti-angiogenic
B
Clusters
Macrophages
T cell
B cell
NK
Stromal
tSNE_1
tSNE_2
Stro 1
Stro 2
Endo
B cell 1
B cell 2
B cell 3
B cell 4
NK 1
NK 2
NK 3
RBC 1
RBC 2
Mphage 1
Mphage 2
Mphage 3
T cell 1
T cell 2
T cell 3
T cell 4
T cell 5
T cell 6
Gr 1
Gr 2
Gr 3
Gr 4
Lin⁻ cells
BM Lin⁻
UCB Lin⁻
AT Lin⁻
C
BM 1
BM 2
UCB 1
UCB 2
AT 1
AT 2
TIMP3
MMP2
CXCL12
TIMP2
ADM
ANG
SFRP1
VEGFD
TIMP1
VEGFB
CTGF
FGF7
IGF1
PDGFD
SFRP2
VEGFC
FGF2
IL6
VEGFA
AAMP
PGF
PTN
ANGPT1
MCP1
IL18
MMP9
BMP6
EDN1
HGF
PDGFC
TMSB4
IL12
IL4
PLG
THBS1
IL1
TGFB1
TNF
Z-Score
1.5
1
0.5
0
-0.5
-1
D
GO Biological Process
BM>AT
AT>BM
Response to VEGF
EC proliferation
VEGF signaling
EC migration
Blood vessel EC migration
Endothelium development
EC chemotaxis
Cell cycle (G1/S)
HSC differentiation
Cell division
Cell cycle (G2/M)
3 2 1 0 1 2 3
- log10 (P-value)
UCB>AT
AT>UCB
Vasculogenesis
Response to VEGF
VEGF signaling
EC migration
EC proliferation
Sprouting angiogenesis
EC migration
Lymphocyte aggregation
Cell-cell adhesion (integrin)
Mucus secretion
Antigen presentation
T cell mediated cytotoxicity
3 2 1 0 1 2 3
- log10 (P-value)

Figure 1: Adipose tissue shows an angiogenic gene profile in single-cell transcriptomics among human stem cell sources

(A) Workflow of scRNA-seq analysis to characterize pro/anti-angiogenic gene profiles of human cell sources.

(B) tSNE map and clustering of 47,035 cells derived from BM, UCB, and AT (left). Distribution of BM, UCB, and AT-Lin$^-$ cells (right).

(C) Heatmap with hierarchical clustering of gene expressions of 38 pro-/anti-angiogenic growth factors in Lin$^-$ cells from human BM, UCB, and AT.

(D) Pathway enrichment analysis between indicated cell sources. The GO terms associated with angiogenesis (red) or overrepresented on BM/UCB (blue) are displayed. See also **Figure S1**.

Figure 2

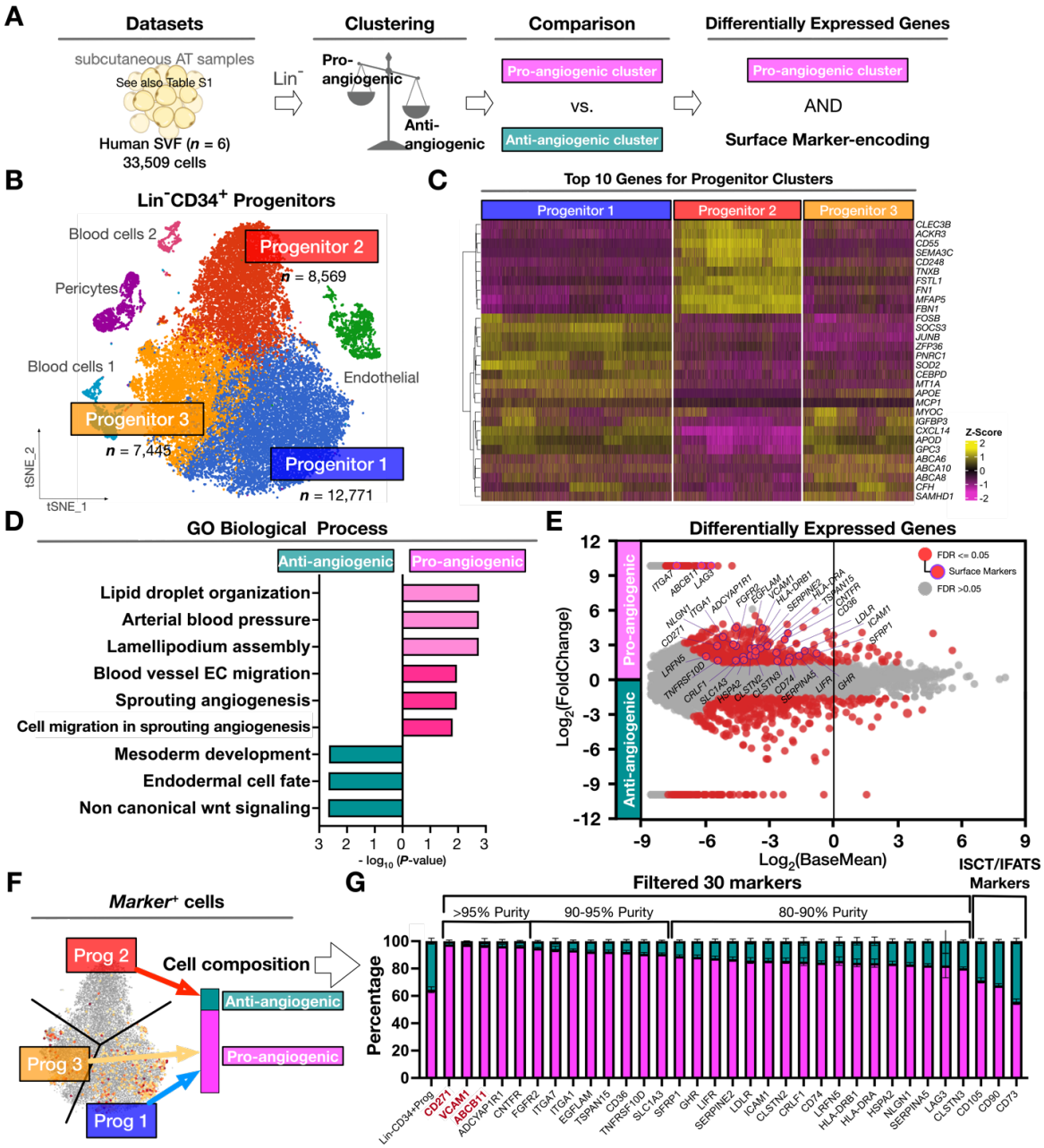
A
Datasets
subcutaneous AT samples
See also Table S1
Human SVF (n = 6)
33,509 cells
Clustering
Lin⁻
Pro-angiogenic
Anti-angiogenic
Comparison
Pro-angiogenic cluster
vs.
Anti-angiogenic cluster
Differentially Expressed Genes
Pro-angiogenic cluster
AND
Surface Marker-encoding
B
Lin⁻CD34⁺ Progenitors
Blood cells 2
Pericytes
Blood cells 1
Progenitor 2
n = 8,569
Endothelial
Progenitor 3
n = 7,445
Progenitor 1
n = 12,771
tSNE_2
tSNE_1
C
Top 10 Genes for Progenitor Clusters
Progenitor 1
Progenitor 2
Progenitor 3
CLEC3B
ACKR3
CD55
SEMA3C
CD248
TNXB
FSTL1
FN1
MFAP5
FBN1
FOSB
SOCS3
JUNB
ZFP36
PNRC1
SOD2
CEBPD
MT1A
APOE
MCP1
MYOC
IGFBP3
CXCL14
APOD
GPC3
ABCA6
ABCA10
ABCA8
CFH
SAMHD1
Z-Score
2
1
0
-1
-2
D
GO Biological Process
Anti-angiogenic
Pro-angiogenic
Lipid droplet organization
Arterial blood pressure
Lamellipodium assembly
Blood vessel EC migration
Sprouting angiogenesis
Cell migration in sprouting angiogenesis
Mesoderm development
Endodermal cell fate
Non canonical wnt signaling
3 2 1 0 1 2 3
- log10 (P-value)
E
Differentially Expressed Genes
Pro-angiogenic
Anti-angiogenic
FDR <= 0.05
Surface Markers
FDR >0.05
Log2(FoldChange)
Log2(BaseMean)
12 9 6 3 0 -3 -6 -9 -12
-9 -6 -3 0 3 6 9
ITGA7
ABCB11
LAG3
ADCYAP1R1
FGFR2
EGFLAM
VCAM1
HLA-DRB1
SERPINE2
HLA-DRA
TSPAN15
CNTFR
CD36
NLGN1
ITGA1
CD271
LDLR
ICAM1
SFRP1
LRFN5
TNFRSF10D
CRLF1
SLC1A3
HSPA2
CLSTN2
CLSTN3
CD74
SERPINA5
LIFR
GHR
ISCT/IFATS Markers
F
Marker⁺ cells
Prog 2
Cell composition
Anti-angiogenic
Pro-angiogenic
Prog 3
Prog 1
G
Filtered 30 markers
>95% Purity
90-95% Purity
80-90% Purity
Percentage
100 80 60 40 20 0
Lin-CD34+Prog
CD271
VCAM1
ABCB11
ADCYAP1R1
CNTFR
FGFR2
ITGA7
ITGA1
EGFLAM
TSPAN15
CD36
TNFRSF10D
SLC1A3
SFRP1
GHR
LIFR
SERPINE2
LDLR
ICAM1
CLSTN2
CRLF1
CD74
LRFN5
HLA-DRB1
HLA-DRA
HSPA2
NLGN1
SERPINA5
LAG3
CLSTN3
CD105
CD90
CD73

Figure 2: Adipose tissue single-cell transcriptomics filters 30 surface markers of angiogenic cluster cells

(A) Diagram illustrating filtering strategy of surface marker genes specific for pro-angiogenic cluster in human SVF.

(B) tSNE map and clustering of 33,509 SVF cells obtained from 6 human subcutaneous AT.

(C) Single-cell heatmap of top 10 marker gens among 3 progenitor clusters (***n*** = 6).

(D) Pathway enrichment analysis between pro-/anti-angiogenic clusters. The top 3 up/downregulated and angiogenesis-related GO terms are displayed (***n*** = 6).

(E) Volcano plot of 2,621 differentially expressed genes between pro/anti-angiogenic clusters. Red dots show differentially expressed genes with $|\log_2(\text{FoldChange})| > 1.5$. Violet circles highlight genes encoding surface proteins (***n*** = 6).

(F) Diagram illustrating the ranking analysis of 30 surface marker genes based on the purity of pro-angiogenic cluster.

(G) Distribution of the pro/anti-angiogenic clusters within the surface marker expressing cell populations (***n*** = 6). Data are presented as the mean ± SEM. See also **Figure S2**.

Figure 3

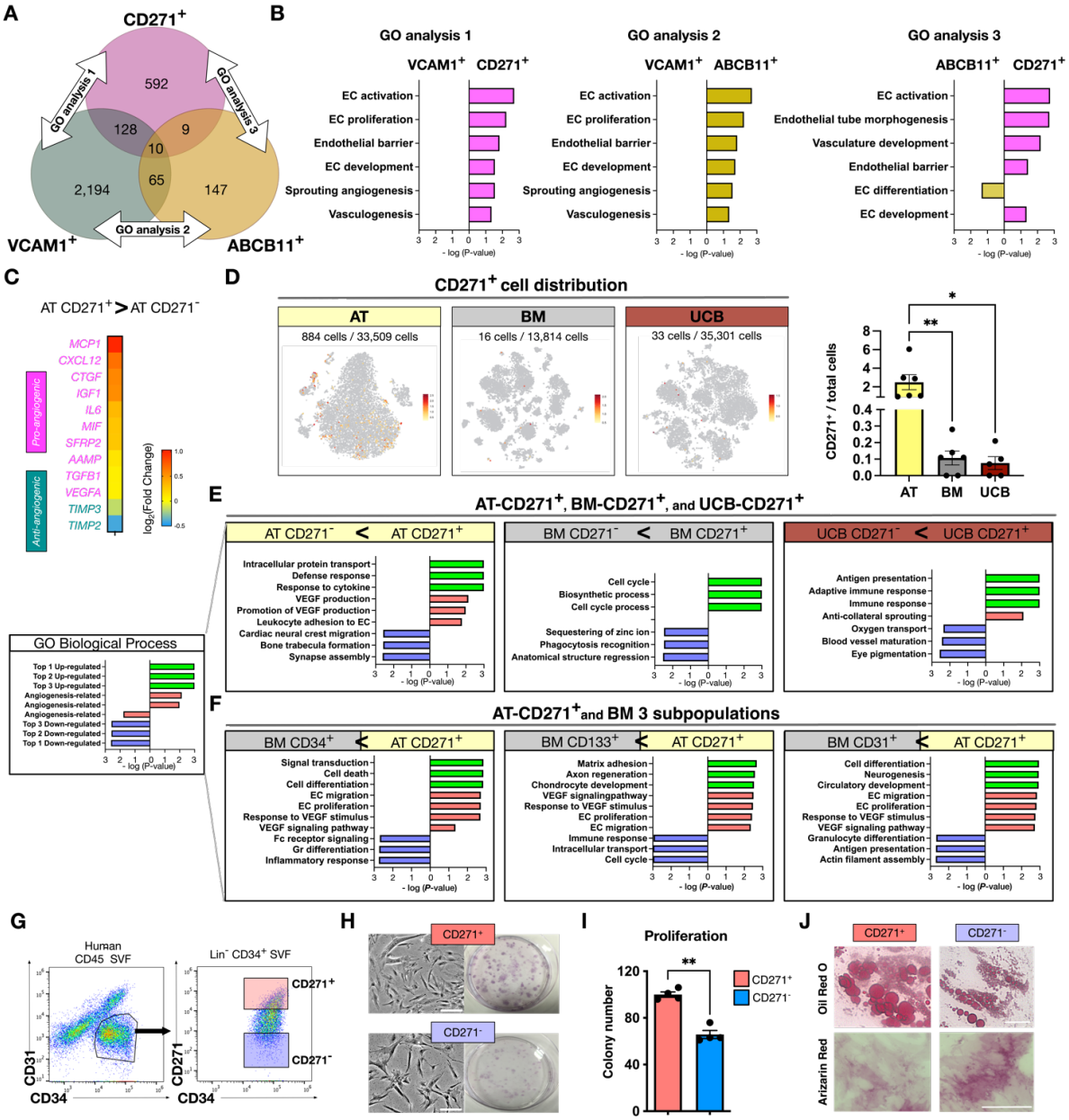
A
CD271+
592
128
9
10
65
2,194
147
GO analysis 1
GO analysis 2
GO analysis 3
VCAM1+
ABCB11+
B
GO analysis 1
VCAM1+ CD271+
EC activation
EC proliferation
Endothelial barrier
EC development
Sprouting angiogenesis
Vasculogenesis
GO analysis 2
VCAM1+ ABCB11+
GO analysis 3
ABCB11+ CD271+
Endothelial tube morphogenesis
Vasculature development
EC differentiation
- log (P-value)
C
AT CD271+ > AT CD271-
MCP1
CXCL12
CTGF
IGF1
IL6
MIF
SFRP2
AAMP
TGFB1
VEGFA
TIMP3
TIMP2
Pro-angiogenic
Anti-angiogenic
log2(Fold Change)
GO Biological Process
Top 1 Up-regulated
Top 2 Up-regulated
Top 3 Up-regulated
Angiogenesis-related
Angiogenesis-related
Angiogenesis-related
Top 3 Down-regulated
Top 2 Down-regulated
Top 1 Down-regulated
D
CD271+ cell distribution
AT
884 cells / 33,509 cells
BM
16 cells / 13,814 cells
UCB
33 cells / 35,301 cells
CD271+ / total cells
E
AT-CD271+, BM-CD271+, and UCB-CD271+
AT CD271- < AT CD271+
Intracellular protein transport
Defense response
Response to cytokine
VEGF production
Promotion of VEGF production
Leukocyte adhesion to EC
Cardiac neural crest migration
Bone trabecula formation
Synapse assembly
BM CD271- < BM CD271+
Cell cycle
Biosynthetic process
Cell cycle process
Sequestering of zinc ion
Phagocytosis recognition
Anatomical structure regression
UCB CD271- < UCB CD271+
Antigen presentation
Adaptive immune response
Immune response
Anti-collateral sprouting
Oxygen transport
Blood vessel maturation
Eye pigmentation
F
AT-CD271+and BM 3 subpopulations
BM CD34+ < AT CD271+
Signal transduction
Cell death
Cell differentiation
EC migration
EC proliferation
Response to VEGF stimulus
VEGF signaling pathway
Fc receptor signaling
Gr differentiation
Inflammatory response
BM CD133+ < AT CD271+
Matrix adhesion
Axon regeneration
Chondrocyte development
VEGF signalingpathway
Response to VEGF stimulus
EC proliferation
EC migration
Immune response
Intracellular transport
Cell cycle
BM CD31+ < AT CD271+
Cell differentiation
Neurogenesis
Circulatory development
EC migration
EC proliferation
Response to VEGF stimulus
VEGF signaling pathway
Granulocyte differentiation
Antigen presentation
Actin filament assembly
- log (P-value)
G
Human CD45 SVF
Lin- CD34+ SVF
CD31
CD34
CD271
CD271+
CD271-
H
CD271+
CD271-
I
Proliferation
Colony number
CD271+
CD271-
J
CD271+
CD271-
Oil Red O
Arizarin Red

Figure 3: Adipose tissue CD271$^+$ cell population is highly angiogenic

(A) Venn diagram illustrating the overlap between CD271$^+$, VCAM1$^+$, and ABCB11$^+$ cells in Lin$^-$CD34$^+$ progenitor cells in AT scRNAseq analysis (***n*** = 6).

(B) Pathway enrichment analysis between CD271$^+$, VCAM1$^+$, and ABCB11$^+$ cell populations.

(C) Heatmap of representative differentially expressed genes of pro-/anti-angiogenic factors between CD271$^+$ and CD271$^-$ cells. The color shows the value of $\log_2$ Fold Change. (***n*** = 6).

(D) The distribution of CD271$^+$ cells in tSNE map and quantification of the frequency of CD271$^+$ cells in AT, BM, and UCB (***n*** = 2/organ). The color of dot plots represents the expression level of CD271.

(E) Pathway enrichment analysis between CD271$^+$ and CD271$^-$ cells in AT, BM, and UCB. The top 3 up/downregulated and angiogenesis-associated GO terms are displayed (***n*** = 2/organ).

(F) Pathway enrichment analysis between AT-CD271$^+$ cells and three BM subpopulations. The top 3 up/downregulated and angiogenesis-associated GO terms are displayed (***n*** = 2/organ).

(G) Representative flow cytometric plots from human subcutaneous AT SVF.

(H) Representative images of cultured ADSCs and generated colonies (Giemsa staining) in CFU assay. Bars = 50 μm.

(I) Colony number in CFU assay of CD271$^+$ and CD271$^-$ ADSCs (***n*** = 4/group).

(J) Representative images of differentiation assays of CD271$^+$ and CD271$^-$ cells. Bars = 100 μm.

Data are presented as the mean ± SEM. ***P*** < 0.05 and ****P*** < 0.01.

Figure 4

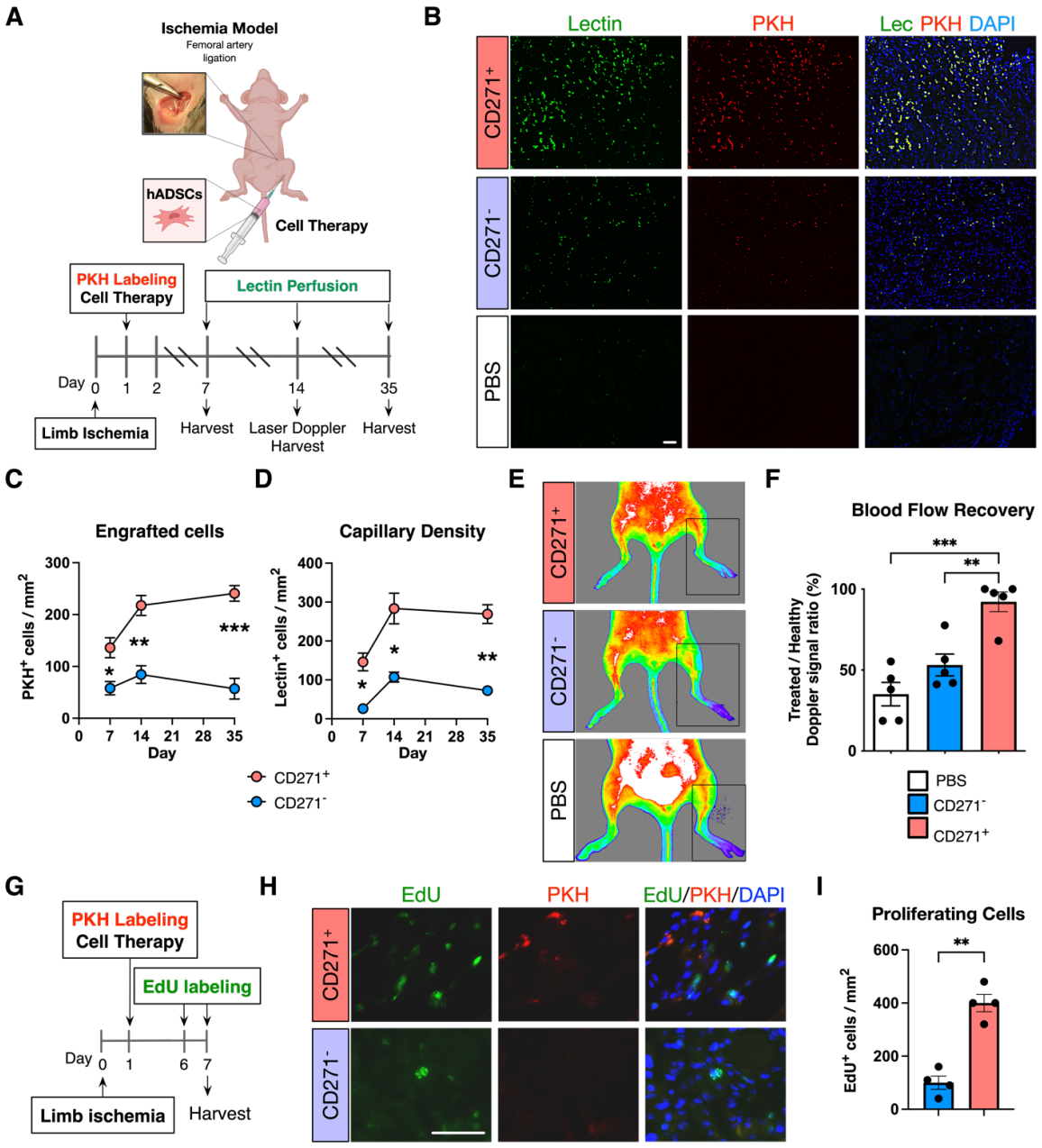
A
Ischemia Model
Femoral artery ligation
hADSCs
Cell Therapy
PKH Labeling Cell Therapy
Lectin Perfusion
Day 0 1 2 7 14 35
Limb Ischemia
Harvest
Laser Doppler Harvest
Harvest
B
Lectin
PKH
Lec PKH DAPI
CD271+
CD271-
PBS
C
Engrafted cells
PKH+ cells / mm2
Day
D
Capillary Density
Lectin+ cells / mm2
Day
CD271+
CD271-
E
CD271+
CD271-
PBS
F
Blood Flow Recovery
Treated / Healthy Doppler signal ratio (%)
PBS
CD271-
CD271+
G
PKH Labeling Cell Therapy
EdU labeling
Day 0 1 6 7
Limb ischemia
Harvest
H
EdU
PKH
EdU/PKH/DAPI
CD271+
CD271-
I
Proliferating Cells
EdU+ cells / mm2

Figure 4: AT-CD271$^+$ progenitors have high *in vivo* angiogenic capacity with long-term engraftment

(A) Diagram of our cell therapy protocol using PKH-labeled human ADSCs and fluorescence-conjugated lectin perfusion.

(B) Representative IHC images for lectin$^+$ capillaries and PKH$^+$ engrafted human ADSCs at day 14 after cell transplantation with either CD271$^+$ or CD271$^-$ progenitors. Bar = 100 μm.

(C) Quantitative analysis of engrafted ADSCs in ischemic limbs on day 7, 14, and 35 with either CD271$^+$ or CD271$^-$ progenitors (***n*** = 5).

(D) Quantitative analysis of capillary density in ischemic limbs on day 7, 14, and 35 (***n*** = 5).

(E) Representative images of laser Doppler analysis at day 14 after cell therapy.

(F) Quantitative analysis of blood flow using laser Doppler analysis at day 14 after cell therapy with either CD271$^+$ or CD271$^-$ progenitors. Signal of treated limb is normalized to signal from healthy limb (set as 100%) (***n*** = 5).

(G) Diagram of cell therapy experiments to evaluate in vivo proliferating cells in ischemic limb after cell therapy.

(H) Representative IHC images for EdU$^+$ cell nuclei and PKH$^+$ engrafted human CD271$^+$ or CD271$^-$ progenitors at day 7 after cell therapy. Bar = 50 μm.

(I) Quantitative analysis of EdU$^+$ proliferating cells after CD271$^+$ or CD271$^-$ progenitor treatment (***n*** = 4). Data are presented as the mean ± SEM. *$P < 0.05$, **$P < 0.01$ and ***$P < 0.005$. See also **Figure S3**.

Figure 5

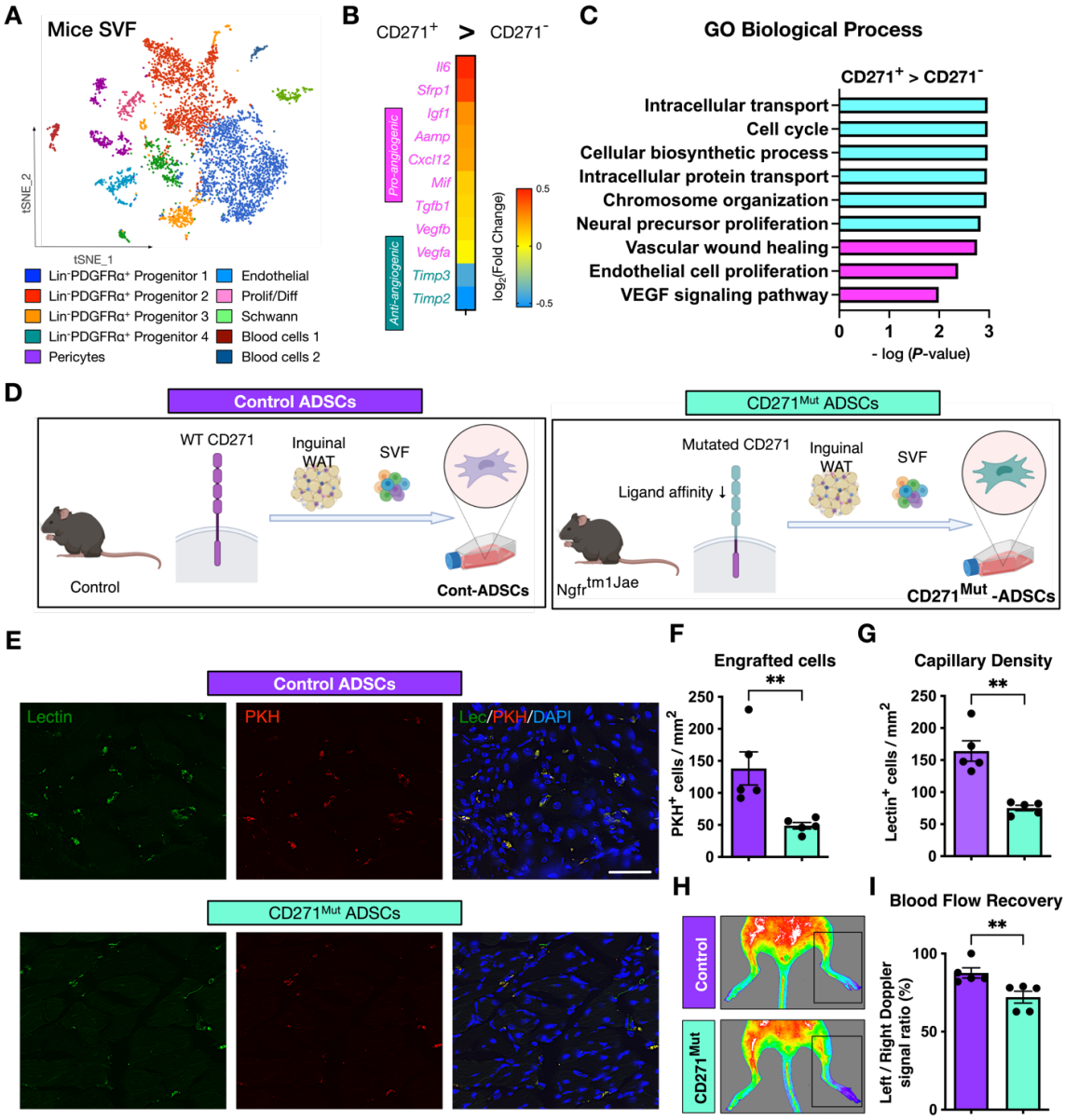
A
Mice SVF
tSNE_1
tSNE_2
Lin⁻PDGFRα⁺ Progenitor 1
Lin⁻PDGFRα⁺ Progenitor 2
Lin⁻PDGFRα⁺ Progenitor 3
Lin⁻PDGFRα⁺ Progenitor 4
Pericytes
Endothelial
Prolif/Diff
Schwann
Blood cells 1
Blood cells 2
B
CD271⁺ > CD271⁻
Il6
Sfrp1
Igf1
Aamp
Cxcl12
Mif
Tgfb1
Vegfb
Vegfa
Timp3
Timp2
Pro-angiogenic
Anti-angiogenic
log2(Fold Change)
0.5
0
-0.5
C
GO Biological Process
CD271⁺ > CD271⁻
Intracellular transport
Cell cycle
Cellular biosynthetic process
Intracellular protein transport
Chromosome organization
Neural precursor proliferation
Vascular wound healing
Endothelial cell proliferation
VEGF signaling pathway
0
1
2
3
- log (P-value)
D
Control ADSCs
WT CD271
Inguinal WAT
SVF
Control
Cont-ADSCs
CD271Mut ADSCs
Mutated CD271
Ligand affinity ↓
Inguinal WAT
SVF
Ngfrtm1Jae
CD271Mut -ADSCs
E
Control ADSCs
Lectin
PKH
Lec/PKH/DAPI
CD271Mut ADSCs
F
Engrafted cells
**
PKH⁺ cells / mm²
250
200
150
100
50
0
G
Capillary Density
**
Lectin⁺ cells / mm²
250
200
150
100
50
0
H
Control
CD271Mut
I
Blood Flow Recovery
**
Left / Right Doppler signal ratio (%)
100
50
0

Figure 5: Normal CD271 activity is required for proangiogenic gene profile and *in vivo* angiogenic capacity of mouse ADSCs

(A) tSNE map and clustering of 4,912 neonatal mouse inguinal fat pad SVF cells.

(B) Heatmap presentation of representative differentially expressed genes of pro/anti-angiogenic factors between $CD271^+$ and $CD271^-$ mouse cells.

(C) Pathway enrichment analysis between mouse $CD271^+$ and $CD271^-$ mouse cells in Lin^- $PDGFR\alpha^+$ progenitors. The top 6 upregulated and angiogenesis-associated GO terms are displayed.

(D) Diagram illustrating preparation of CD271-mutated mouse-derived ($CD271^{Mut}$) and littermate wild-type mouse-derived (Control) ADSCs.

(E) Representative IHC images of $lectin^+$ capillaries and PKH^+ engrafted mouse ADSCs on day 14 after cell transplantation with either $CD271^{Mut}$ or control ADSCs. Bar = 50 μm.

(F) Quantitative analysis of engrafted ADSCs in ischemic limbs on day 14 after treatment with $CD271^{Mut}$ or control ADSCs. (***n***=5)

(G) Quantitative analysis of capillary density in ischemic limbs on day 14 after treatment with $CD271^{Mut}$ or control ADSCs. (***n***=5)

(H) Representative images of laser Doppler analysis on day 14 after transplantation with $CD271^{Mut}$ or control ADSCs following limb ischemia induction (***n*** = 5).

(I) Quantitative analysis of blood flow using laser Doppler analysis at day 14 after cell therapy with either $CD271^{Mut}$ or control ADSCs. Signal of treated limb is normalized to signal from healthy limb (set as 100%). Data are presented as the mean ± SEM. ***P*** < 0.05 and ****P*** < 0.01. See also **Figure S4**.

Figure 6

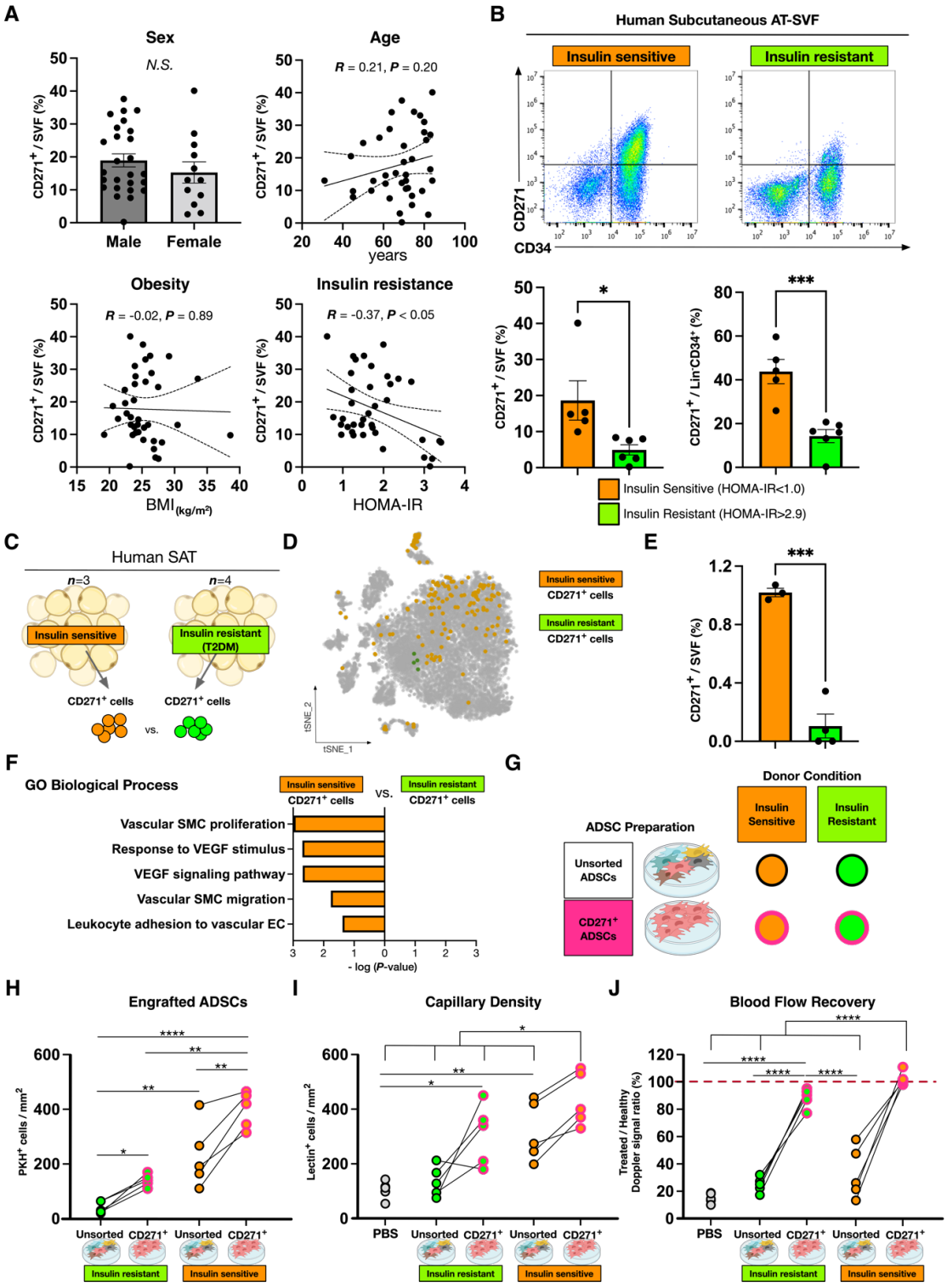
A
Sex
N.S.
CD271+ / SVF (%)
Male
Female
Age
R = 0.21, P = 0.20
years
Obesity
R = -0.02, P = 0.89
BMI (kg/m²)
Insulin resistance
R = -0.37, P < 0.05
HOMA-IR
B
Human Subcutaneous AT-SVF
Insulin sensitive
Insulin resistant
CD271
CD34
CD271+ / Lin-CD34+ (%)
Insulin Sensitive (HOMA-IR<1.0)
Insulin Resistant (HOMA-IR>2.9)
C
Human SAT
n=3
n=4
Insulin sensitive
Insulin resistant (T2DM)
CD271+ cells
vs.
D
tSNE_1
tSNE_2
E
F
GO Biological Process
Vascular SMC proliferation
Response to VEGF stimulus
VEGF signaling pathway
Vascular SMC migration
Leukocyte adhesion to vascular EC
- log (P-value)
G
Donor Condition
ADSC Preparation
Unsorted ADSCs
CD271+ ADSCs
H
Engrafted ADSCs
PKH+ cells / mm²
I
Capillary Density
Lectin+ cells / mm²
J
Blood Flow Recovery
Treated / Healthy Doppler signal ratio (%)
PBS
Unsorted
CD271+

Figure 6: AT-CD271$^+$ progenitors are decreased and impaired in insulin resistant donors
(A) Plots comparing CD271$^+$ cell frequency in SVF (CD271$^+$/SVF) and clinical parameters of CVD patients with or without insulin resistance (***n*** = 38).
(B) Representative flow cytometric plots and comparative analysis of CD271$^+$ cell abundance in total SVF or Lin$^-$CD34$^+$ SVF of CVD patients with or without insulin resistance (***n*** = 5-6).
(C) Diagram illustrating human AT samples used for scRNA-seq analysis
(D) Distribution of CD271$^+$ cells in tSNE map derived from lean healthy (***n*** = 3, insulin sensitive, **blue dots**) and obese-diabetic patients (***n*** = 4, insulin resistant, **red dots**).
(E) Comparative analysis of the percentage of CD271$^+$ cells between patients with and without insulin resistance in the scRNA-seq analysis (***n*** = 3-4).
(F) Pathway enrichment analysis between CD271$^+$ cells from patients with and without insulin resistance. GO terms associated with angiogenesis are displayed.
(G) Diagram illustrating ADSC groups for cell therapy experiments stratified by donor types and ADSC preparation methods (unsorted and CD271$^+$ ADSCs).
(H) Quantitative analysis of engrafted ADSCs and capillary density in ischemic limbs at day 14 after cell therapy (***n*** = 5). The red-colored dashed line indicates complete recovery of blood flow (100%). *$P < 0.05$, **$P < 0.01$, ***$P < 0.005$, and ****$P < 0.001$. See also **Figure S6**.

Figure 7

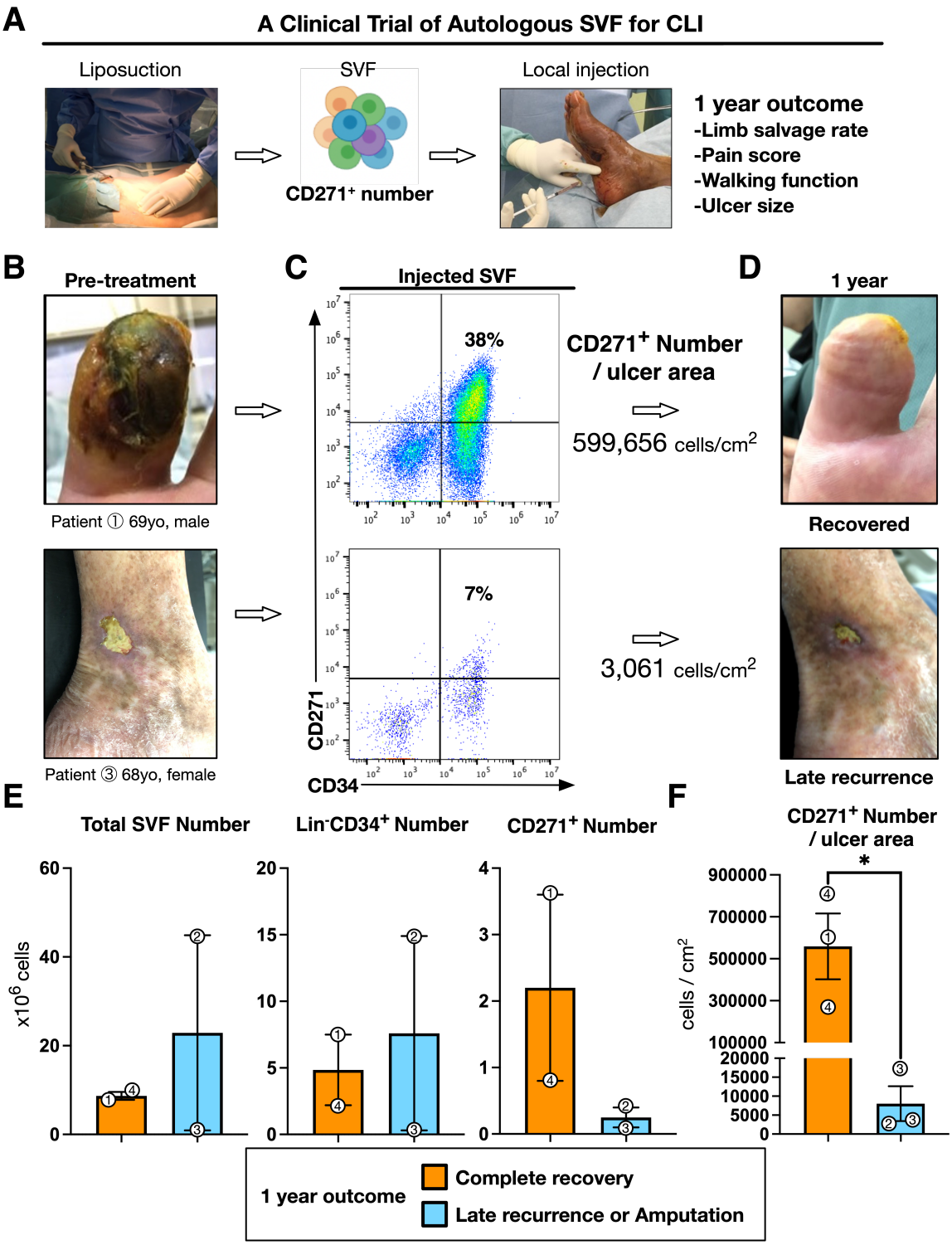
A
A Clinical Trial of Autologous SVF for CLI
Liposuction
SVF
Local injection
CD271+ number
1 year outcome
-Limb salvage rate
-Pain score
-Walking function
-Ulcer size
B
Pre-treatment
Patient ① 69yo, male
Patient ③ 68yo, female
C
Injected SVF
38%
7%
CD271
CD34
CD271+ Number / ulcer area
599,656 cells/cm2
3,061 cells/cm2
D
1 year
Recovered
Late recurrence
E
Total SVF Number
Lin-CD34+ Number
CD271+ Number
x10^6 cells
F
CD271+ Number / ulcer area
cells / cm2
*
1 year outcome
Complete recovery
Late recurrence or Amputation

Figure 7: The number of AT-CD271$^+$ progenitors injected was significantly higher in patients who completely recovered from CLI in SVF therapy

(A) Diagram of the study design of a clinical trial of autologous SVF transplantation for CLI.

(B) Representative images of CLI lesions prior to autologous SVF transplantation.

(C) Representative flow cytometric analysis of autologous SVF transplantation.

(D) Representative images of CLI lesions acquired 12 months after autologous SVF transplantation.

(E) Quantification of total SVF, Lin$^-$CD34$^+$, and CD271$^+$ cell numbers injected to CLI patients ($\boldsymbol{n}$ = 4)

(F) Quantification of the number of CD271$^+$ cells per ulcer area between patients ($\boldsymbol{n}$ = 4 patients, $\boldsymbol{n}$ = 6 ulcer lesions). Numbers within data point indicates patient identification number. Data are represented as the mean ± SEM. *$\boldsymbol{P}$ < 0.05. See also **Figure S7** and **Table S7**.

METHODS

RESOURCE AVAILABILITY

Lead contact

Further information and requests for resources and reagents will be fulfilled by the lead contact, Masayuki Takamura (mtakamura@staff.kanazawa-u.ac.jp)

Materials availability

None of unique reagents were generated in this study.

Data and code availability

Single-cell RNA-seq datasets analyzed in this study are available at NCBI Gene Expression Omnibus (GEO). GEO accession numbers are listed in **Table S1**. Any information and Seurat analysis files required to reanalyze the data reported in this study is available from the Lead Contact upon request.

EXPERIMENTAL MODEL AND SUBJECT DETAILS

Study Design and Patient Population

In the study of patient-derived AT and SVF, eligible patients were adult males or females with CVD who underwent elective cardiac surgery, including coronary artery bypass grafting (CABG) and cardiac valve replacement/plastic surgeries. Major exclusion criteria were acute emergency diseases, including acute myocardial infarction, active and acute infectious disease, uncontrolled diabetes mellitus (HbA1c > 8.0%), hypo/hyperinsulinemia (< 2.2 or > 13.0 μU/mL), systemic inflammatory disease (autoimmune disease), and history of irradiation therapy at tissue harvest sites. Thirty-eight patients were enrolled between April 2017 and February 2022. This study was registered in the University Hospital Medical Information Network Center (UMIN, Tokyo, Japan) Clinical Trials Registration System as UMIN000020764. After enrollment with written informed consent, clinical and laboratory variables were collected preoperatively, and all data were blinded for the researchers who performed further experiments.

The detailed protocol and eligibility for the clinical trial of SVF therapy for CLI are published,[46,64] Briefly, this was a multicenter clinical trial to investigate the feasibility and safety of SVF injection for CLI patients with no option for treatment[46]. Autologous SVF from

liposuction was transplanted to the ulcer lesions via intra-muscular injections. The safety, feasibility, and the efficacy including hard outcomes, including survival rate and amputation free rate in 6 months, of SVF therapy were investigated. In this study, we sub-analyzed 4 patients (**Table S6**) on whom we performed cell therapy in our institution (Kanazawa University) with 1-year follow-up data. On the remaining samples after SVF injection, we analyzed their viability and surface antigen expressions.

The studies using human samples subjects was performed according to Declaration of Helsinki principles and approved by the Research Ethics Board of the University of Kanazawa. Written informed consent was obtained from all patients prior to inclusion in the study. All animal experiments were approved by the Institution for Experimental Animals of the Kanazawa University Advanced Science Research Center.

Mice

All animal protocols were approved and performed according to the Guide for the Care and Use of Laboratory Animals of Kanazawa University, which strictly conforms to the Guide for the Care and Use of Laboratory Animals published by the US National Institutes of Health (NIH, Bethesda, MD, USA). Athymic nude mice for xenograft experiments were purchased from the Charles River Laboratories. Heterozygous $Ngfr^{tm1jae41}$ were purchased from the Jackson Laboratory (Strain #002213) and crossed two- or three-times with C57BL/6J females before generating homozygous $Ngfr^{tm1Jae}$ ($CD271^{Mut}$) mice. Homozygous $Ngfr^{tm1Jae}$ and controls mice were used at 6–8-week-old) before they develop peripheral nervous denervation and cutaneous ulcers (16 weeks old).

Cell Therapy Model of Limb Ischemia

6- to 8-week-old athymic nude mice (Jackson Laboratory) were subjected to hindlimb ischemia. Mice were anesthetized by intraperitoneal injection of sodium pentobarbital (40 mg/kg). The proximal portion of the left femoral artery was resected. After 24 h, 0.5 million human ADSCs at passage 4-6 were prepared for injection. In brief, ADSCs were harvested by trypsinization, labeled with PKH26 cell linker dye (2 μ L/mL, 3 minutes in room temperature, Sigma), and resuspended in PBS (5.0×10^5 cells in 60 μ l with 27 gauge syringes). Labeled ADSCs were immediately injected intra-muscularly at three different sites (gastrocnemius, gracilis, and quadriceps muscles, 20 µl per injection). Sham-operated mice were injected with PBS and used as a control group. At day 7, 14, and 35 after cell therapy, mice were anesthetized and subjected to laser Doppler analysis for blood flow, followed by harvest of gastrocnemius muscles.

METHOD DETAILS

Single-Cell Transcriptome Datasets and Analysis

We used scRNA-seq datasets of AT,[25,65,66] BM,[23,67] and UCB.[24,68] Gene Expression Omnibus (GEO) accession numbers of revisited datasets are listed in **Table S1**. For quality control, cells expressing < 200 genes and with a mitochondrial content > 5% were removed. For batch integration of multiple scRNAseq datasets, Harmony was used to remove the batch effect.[69] After data normalization, dimension reduction (tSNE) and clustering with using a Louvain algorism were performed. Marker gene analysis and differential expression (DE) analysis were performed using non-parametric approach, Venice[70] or DESeq2. The Gene Set Enrichment Analysis (GSEA) was performed to list GO Biological Process terms.[71] Cluster annotation was determined according to marker genes for clusters identified by non-parametric approach, Venice and collation with overlapping genes from the Human Cell Atlas and previously published scRNA-seq reports.[19,20] These analyses were performed in BioTuring Browser 3.[72]

Adipose Tissue and SVF Processing

Unnecessary subcutaneous adipose tissues (1-2 gram) discarded during making surgical incision were obtained. SVF cells were isolated from adipose tissue using a procedure modified from Zuk et al.[38] Briefly, adipose tissue was digested by Liberase TM Research Grade collagenase solution (0.4 units/mL; Sigma-Aldrich) for 30 min using gentleMACS Dissociator ("ATDK" program, Miltenyi Biotec). Then, the digested solution was filtered through a 100-µm cell strainer (BD Biosciences) to remove undigested connective tissue debris. After centrifugation (400g, 10 minutes at room temperature), the supernatant containing mature adipocytes was discarded. The pellet was lysed to deplete erythrocytes with BD Pharm Lyse (2mL for 1 minute at room temperature, BD Biosciences) and washed twice with phosphate-buffered saline (PBS) with 2.0% fetal bovine serum (FBS). The final pellet was resuspended in 150 μL of autoMACS Running buffer (Miltenyi) and counted with a hemocytometer in triplicate.

Flow Cytometry and Sorting

SVF cells were separated into $CD45^+$ and $CD45^-$ cells using microbeads and autoMACS pro separator (Miltenyi) according to the manufacturer's instructions. $CD45^-$ cells were incubated with Fc Block (BD Biosciences) prior to staining. Then, cells were labeled with following antibodies: human CD31-FITC (BD Biosciences, clone WM59, used in 1:20 dilution), CD271-APC (Miltenyi, cloneME20.4-1.H4, 1:20), and CD34-peridinin chlorophyll protein (PerCP) (BD Biosciences, clone 8G12, 1:20) for 15 min at 4°C. Then, cells were washed twice in PBS with

2.0% FBS. Flow cytometric data were acquired by using Accuri C6 (BD Biosciences). Before immunophenotyping, the instrument performance was validated by using BD Accuri Spherotech Validation Beads (BD Biosciences). A total of 30,000-100,000 events were acquired at slow flow rate. Acquired data were analyzed using FlowJo software X 10.0.7 (Tree Star Inc.). Isotype-matched negative controls or fluorescence-minus controls were used to define the threshold for each specific signal and establish the appropriate gate for positive cells.

Cell Culture

The $CD45^-$ stromal cells that remained from flow cytometric analysis were seeded at a density of 1.0×10^4 cells/cm^2. Cells were cultured in standard conditions (5% carbon dioxide, 37°C) in DMEM/F12 (Thermo Fisher Scientific) supplemented with 10% FBS and 1% antibiotic-antimycotic (Thermo Fisher Scientific) solution. At 24 h after seeding, non-adherent cells were removed by washing the plates, and then medium was changed every three days. ADSCs were harvested at sub-confluency with trypsin (0.05% trypsin-EDTA; Thermo Fisher Scientific). Cells at the second passage and thereafter were replated at a density of 3,000 cells/cm2.

RT-qPCR

Total RNA was isolated from ADSCs using RNeasy Mini Kit (Qiagen). Total RNA (100 ng) was used to generate cDNA using the TaqMan Universal Master Mix (Applied Biosystems). Quantitative real-time polymerase chain reaction (qRT-PCR) analysis was performed on an ABI Prism 7300 sequence detection system (Applied Biosystems). The TaqMan probes (Applied Biosystems) used in this study were listed in **Table S7**. Relative expression was assessed by comparative CT method, correcting for amplification efficiency of the primers, and performed in duplicate.

Colony-Forming Unit Assay

Cultured AT-$CD271^+$ or $CD271^-$ progenitors at passage 4 were used for colony-forming unit (CFU) assays. Cells were detached and plated at a density of 20 cells/cm^2 in 10 cm dishes. Half the medium was changed at day 7 after plating. Adherent cell clusters of greater than 50 cells were counted at day 14 with Giemsa staining. The experiments were performed in triplicate for each sample.

Flow Cytometry of ADSC treated limb

At 14 days after cell therapy in xenograft model, gastrocnemius muscle was harvested and digested using gentleMACS (Miltenyi) with “m_muscle_01” program and Liberase TM solution. Single cells from digested limb were filtered through 40 μ m cell strainer and labeled with

immunofluorescence-conjugated antibodies; mice CD31-PerCP-$Cy^{5.5}$ (BD Bioscience, clone MEC 13.3, 1:20), human CD31-FITC (BD Biosciences, clone WM59), human CD271-APC (Miltenyi, cloneME20.4-1.H4, 1:20), human CD90-APC (BD Biosciences, clone 5E10), and human CD105-PerCP-$Cy^{5.5}$ (BD Biosciences, clone 266, 1:20) for 15 min at 4°C. Flow cytometric data was acquired by similar methods described above in *Flow Cytometry and Sorting* section.

Blood Flow Measurement

Blood flow was assessed using Laser Doppler blood flow imager (OZ-2 LCB, OMEGAWAVE, Japan) at day 1, 3, and 14 after induction of limb ischemia. Before scanning, mice were placed on a heating plate at 37°C for 15 min, followed by anesthetization using intraperitoneal injection of sodium pentobarbital (20 mg/kg). The signal intensities basically reflecting laser scattering by red blood cells within circulation were obtained as blood flow value. The mean blood flow value was acquired in region of interest (ROI) capturing the whole mouse lower limb. The ratio of blood flow values of the ischemic (left) limb to the healthy (right) limb were calculated as blood flow recovery to avoid data variations caused by ambient light and temperature.[8,9]

In Vivo Proliferation Assay

EdU solution (5mg/2mL) was administered via intra-peritoneal injection at day 6 after ADSC therapy. At day 7, the gastrocnemius muscles were harvested and processed to frozen sections. EdU positive nucleus were detected using EdU *in vivo* imaging kits (BCK488-IV-IM, baseclick) according to the manufacturer's instruction. The number of EdU^+ and $DAPI^+$ nucleus was counted in frozen sections in duplicate.

Immunohistochemistry

Tissue vascularization and ADSCs engraftment were evaluated at day 14 and 35. Mice were anesthetized and injected with 50 μg of FITC-conjugated isolectin B4 (FL-1201, Vector Laboratories) via tail vein. After 10 min, mice were perfused with PBS for 3 min to remove unbound isolectin B4 in the blood vessels, and perfusion-fixed with 4% paraformaldehyde. The gastrocnemius muscles were removed, fixed with 4% paraformaldehyde at 4°C overnight, and incubated in 30% sucrose solution for 24 hours. Frozen sections of the tissue were obtained at 10 μm thickness and counterstained with DAPI. Capillary density and engraftment of injected ADSCs were analyzed by counting FITC and PKH positive cells, respectively, in five randomly selected fields per section. The experiments were performed in duplicate or triplicate for each human ADSCs sample.

Statistics

Continuous data are expressed as the mean ± SEM, and statistical analysis was performed with Prism 9 software (GraphPad, USA). Group comparisons were performed using paired or unpaired *t* tests or one-way analysis of variance (ANOVA). Correlation analysis was performed using Pearson correlation for normally distributed data (Shapiro–Wilk normality test) or Spearman correlation for nonnormally distributed data. Statistical significance was defined as $^{*}\boldsymbol{P} < 0.05$, $^{**}\boldsymbol{P} < 0.01$, $^{***}\boldsymbol{P} < 0.005$ and $^{****}\boldsymbol{P} < 0.001$. All reported statistical tests were two-tailed.

REFERENCES

1. Roth, G.A., Johnson, C., Abajobir, A., Abd-Allah, F., Abera, S.F., Abyu, G., Ahmed, M., Aksut, B., Alam, T., Alam, K., et al. (2017). Global, Regional, and National Burden of Cardiovascular Diseases for 10 Causes, 1990 to 2015. Journal of the American College of Cardiology *70*, 1-25. 10.1016/j.jacc.2017.04.052.
2. Norgren, L., Hiatt, W.R., Dormandy, J.A., Nehler, M.R., Harris, K.A., Fowkes, F.G., and Rutherford, R.B. (2007). Inter-society consensus for the management of peripheral arterial disease. International angiology : a journal of the International Union of Angiology *26*, 81-157. 10.1016/j.jvs.2006.12.037.
3. Lawall, H., Bramlage, P., and Amann, B. (2011). Treatment of peripheral arterial disease using stem and progenitor cell therapy. Journal of Vascular Surgery *53*, 445-453. 10.1016/j.jvs.2010.08.060.
4. Annex, B.H. (2013). Therapeutic angiogenesis for critical limb ischaemia. Nature Reviews Cardiology *10*, 387-396. 10.1038/nrcardio.2013.70.
5. Samsonraj, R.M., Raghunath, M., Nurcombe, V., Hui, J.H., van Wijnen, A.J., and Cool, S.M. (2017). Concise Review: Multifaceted Characterization of Human Mesenchymal Stem Cells for Use in Regenerative Medicine. Stem Cells Translational Medicine *6*, 2173-2185. 10.1002/sctm.17-0129.
6. Gnecchi, M., Zhang, Z., Ni, A., and Dzau, V.J. (2008). Paracrine mechanisms in adult stem cell signaling and therapy. Circ Res *103*, 1204-1219. 10.1161/circresaha.108.176826.
7. Qadura, M., Terenzi, D.C., Verma, S., Al-Omran, M., and Hess, D.A. (2018). Concise Review: Cell Therapy for Critical Limb Ischemia: An Integrated Review of Preclinical and Clinical Studies. Stem Cells, 161-171. 10.1002/stem.2751.
8. Miranville, A. (2004). Improvement of Postnatal Neovascularization by Human Adipose Tissue-Derived Stem Cells. Circulation *110*, 349-355. 10.1161/01.CIR.0000135466.16823.D0.
9. Barros, S.D., Dehez, S., Arnaud, E., Barreau, C., Cazavet, A., Perez, G., Galinier, A., Casteilla, L., and Planat-Bénard, V. (2013). Aging-related Decrease of Human ASC Angiogenic Potential Is Reversed by Hypoxia Preconditioning Through ROS Production. Molecular Therapy *21*, 399-408. 10.1038/mt.2012.213.
10. Beltrán-Camacho, L., Rojas-Torres, M., and Durán-Ruiz, M.C. (2021). Current status of angiogenic cell therapy and related strategies applied in critical limb ischemia. International Journal of Molecular Sciences *22*, 1-27. 10.3390/ijms22052335.
11. Kim, H., Cho, H.-J., Kim, S.-W., Liu, B., Choi, Y.J., Lee, J., Sohn, Y.-D., Lee, M.-Y., Houge, M.a., and Yoon, Y.-s. (2010). CD31+ cells represent highly angiogenic and vasculogenic cells in bone marrow: novel role of nonendothelial CD31+ cells in neovascularization and their therapeutic effects on ischemic vascular disease. Circulation research *107*, 602-614. 10.1161/CIRCRESAHA.110.218396.
12. Rigato, M., Monami, M., and Fadini, G.P. (2017). Autologous Cell Therapy for Peripheral Arterial Disease. Circulation Research *120*, 1326-1340. doi:10.1161/CIRCRESAHA.116.309045.
13. Chiang, K.J., Chiu, L.C., Kang, Y.N., and Chen, C. (2021). Autologous stem cell therapy for chronic lower

extremity wounds: A meta-analysis of randomized controlled trials. Cells *10*, 1-17. 10.3390/cells10123307.

14. Losordo, D.W., Kibbe, M.R., Mendelsohn, F., Marston, W., Driver, V.R., Sharafuddin, M., Teodorescu, V., Wiechmann, B.N., Thompson, C., Kraiss, L., et al. (2012). A randomized, controlled pilot study of autologous CD34+ cell therapy for critical limb ischemia. Circulation: Cardiovascular Interventions *5*, 821-830. 10.1161/CIRCINTERVENTIONS.112.968321.
15. Fang, Y., Wei, Z., Chen, B., Pan, T., Gu, S., Liu, P., Guo, D., Xu, X., Jiang, J., Yang, J., et al. (2018). A Five-Year Study of the Efficacy of Purified CD34+ Cell Therapy for Angiitis-Induced No-Option Critical Limb Ischemia. STEM CELLS Translational Medicine *7*, 583-590. 10.1002/sctm.17-0252.
16. Raval, A.N., Schmuck, E.G., Tefera, G., Leitzke, C., Ark, C.V., Hei, D., Centanni, J.M., de Silva, R., Koch, J., Chappell, R.G., and Hematti, P. (2014). Bilateral administration of autologous CD133+ cells in ambulatory patients with refractory critical limb ischemia: lessons learned from a pilot randomized, double-blind, placebo-controlled trial. Cytotherapy *16*, 1720-1732. 10.1016/j.jcyt.2014.07.011.
17. Etzrodt, M., Endele, M., and Schroeder, T. (2014). Quantitative single-cell approaches to stem cell research. Cell Stem Cell *15*, 546-558. 10.1016/j.stem.2014.10.015.
18. Wilson, N.K., Kent, D.G., Buettner, F., Shehata, M., Macaulay, I.C., Calero-Nieto, F.J., Sánchez Castillo, M., Oedekoven, C.A., Diamanti, E., Schulte, R., et al. (2015). Combined Single-Cell Functional and Gene Expression Analysis Resolves Heterogeneity within Stem Cell Populations. Cell Stem Cell *16*, 712-724. 10.1016/j.stem.2015.04.004.
19. Han, X., Zhou, Z., Fei, L., Sun, H., Wang, R., Chen, Y., Chen, H., Wang, J., Tang, H., Ge, W., et al. (2020). Construction of a human cell landscape at single-cell level. Nature *581*, 303-309. 10.1038/s41586-020-2157-4.
20. Emont, M.P., Jacobs, C., Essene, A.L., Pant, D., Tenen, D., Colleluori, G., Di Vincenzo, A., Jørgensen, A.M., Dashti, H., Stefek, A., et al. (2022). A single-cell atlas of human and mouse white adipose tissue. Nature. 10.1038/s41586-022-04518-2.
21. Deng, Q., Han, G., Puebla-Osorio, N., Ma, M.C.J., Strati, P., Chasen, B., Dai, E., Dang, M., Jain, N., Yang, H., et al. (2020). Characteristics of anti-CD19 CAR T cell infusion products associated with efficacy and toxicity in patients with large B cell lymphomas. Nature Medicine *26*, 1878-1887. 10.1038/s41591-020-1061-7.
22. Rabilloud, T., Potier, D., Pankaew, S., Nozais, M., Loosveld, M., and Payet-Bornet, D. (2021). Single-cell profiling identifies pre-existing CD19-negative subclones in a B-ALL patient with CD19-negative relapse after CAR-T therapy. Nature Communications *12*, 865. 10.1038/s41467-021-21168-6.
23. Muto, T., Guillamot, M., Yeung, J., Fang, J., Bennett, J., Nadorp, B., Lasry, A., Redondo, L.Z., Choi, K., Gong, Y., et al. (2022). TRAF6 functions as a tumor suppressor in myeloid malignancies by directly targeting MYC oncogenic activity. Cell Stem Cell *29*, 298-314.e299. 10.1016/j.stem.2021.12.007.
24. Luo, O.J., Lei, W., Zhu, G., Ren, Z., Xu, Y., Xiao, C., Zhang, H., Cai, J., Luo, Z., Gao, L., et al. (2022). Multidimensional single-cell analysis of human peripheral blood reveals characteristic features of the

immune system landscape in aging and frailty. Nature Aging *2*, 348-364. 10.1038/s43587-022-00198-9.

25. Hildreth, A.D., Ma, F., Wong, Y.Y., Sun, R., Pellegrini, M., and O'Sullivan, T.E. (2021). Single-cell sequencing of human white adipose tissue identifies new cell states in health and obesity. Nat Immunol *22*, 639-653. 10.1038/s41590-021-00922-4.
26. He, S., Wang, L.-H., Liu, Y., Li, Y.-Q., Chen, H.-T., Xu, J.-H., Peng, W., Lin, G.-W., Wei, P.-P., Li, B., et al. (2020). Single-cell transcriptome profiling of an adult human cell atlas of 15 major organs. Genome Biology *21*, 294. 10.1186/s13059-020-02210-0.
27. Karlsson, M., Zhang, C., Méar, L., Zhong, W., Digre, A., Katona, B., Sjöstedt, E., Butler, L., Odeberg, J., Dusart, P., et al. (2021). A single–cell type transcriptomics map of human tissues. Science Advances *7*, eabh2169. doi:10.1126/sciadv.abh2169.
28. Banas, A., Teratani, T., Yamamoto, Y., Tokuhara, M., Takeshita, F., Osaki, M., Kawamata, M., Kato, T., Okochi, H., and Ochiya, T. (2008). IFATS collection: in vivo therapeutic potential of human adipose tissue mesenchymal stem cells after transplantation into mice with liver injury. Stem cells (Dayton, Ohio) *26*, 2705-2712. 10.1634/stemcells.2008-0034.
29. Kim, H., Cho, H.J., Kim, S.W., Liu, B., Choi, Y.J., Lee, J., Sohn, Y.D., Lee, M.Y., Houge, M.A., and Yoon, Y.S. (2010). CD31+ cells represent highly angiogenic and vasculogenic cells in bone marrow: Novel role of nonendothelial CD31+ cells in neovascularization and their therapeutic effects on ischemic vascular disease. Circulation Research *107*, 602-614. 10.1161/CIRCRESAHA.110.218396.
30. Gincberg, G., Shohami, E., Lazarovici, P., and Elchalal, U. (2018). Human Umbilical Cord Blood CD45(+) Pan-Hematopoietic Cells Induced a Neurotherapeutic Effect in Mice with Traumatic Brain Injury: Immunophenotyping, Comparison of Maternal and Neonatal Parameters, and Immunomodulation. J Mol Neurosci *64*, 185-199. 10.1007/s12031-017-1008-8.
31. Ratajczak, M.Z., Kucia, M., Jadczyk, T., Greco, N.J., Wojakowski, W., Tendera, M., and Ratajczak, J. (2012). Pivotal role of paracrine effects in stem cell therapies in regenerative medicine: can we translate stem cell-secreted paracrine factors and microvesicles into better therapeutic strategies? Leukemia *26*, 1166-1173. 10.1038/leu.2011.389.
32. Xu, L., Kanasaki, K., Kitada, M., and Koya, D. (2012). Diabetic angiopathy and angiogenic defects. Fibrogenesis & Tissue Repair *5*, 13. 10.1186/1755-1536-5-13.
33. Logsdon, E.A., Finley, S.D., Popel, A.S., and Gabhann, F.M. (2014). A systems biology view of blood vessel growth and remodelling. Journal of Cellular and Molecular Medicine *18*, 1491-1508. https://doi.org/10.1111/jcmm.12164.
34. Madu, C.O., Wang, S., Madu, C.O., and Lu, Y. (2020). Angiogenesis in Breast Cancer Progression, Diagnosis, and Treatment. Journal of Cancer *11*, 4474-4494. 10.7150/jca.44313.
35. Traktuev, D.O., Merfeld-Clauss, S., Li, J., Kolonin, M., Arap, W., Pasqualini, R., Johnstone, B.H., and March, K.L. (2008). A population of multipotent CD34-positive adipose stromal cells share pericyte and mesenchymal surface markers, reside in a periendothelial location, and stabilize endothelial networks.

Circulation Research *102*, 77-85. 10.1161/CIRCRESAHA.107.159475.

36. Bourin, P., Bunnell, B.a., Casteilla, L., Dominici, M., Katz, A.J., March, K.L., Redl, H., Rubin, J.P., Yoshimura, K., and Gimble, J.M. (2013). Stromal cells from the adipose tissue-derived stromal vascular fraction and culture expanded adipose tissue-derived stromal/stem cells: A joint statement of the International Federation for Adipose Therapeutics and Science (IFATS) and the International So. Cytotherapy *15*, 641-648. 10.1016/j.jcyt.2013.02.006.
37. Mabuchi, Y., Morikawa, S., Harada, S., Niibe, K., Suzuki, S., Renault-Mihara, F., Houlihan, D.D., Akazawa, C., Okano, H., and Matsuzaki, Y. (2013). LNGFR+THY-1+VCAM-1hi+ Cells Reveal Functionally Distinct Subpopulations in Mesenchymal Stem Cells. Stem Cell Reports *1*, 152-165. 10.1016/j.stemcr.2013.06.001.
38. Zuk, P.A., Zhu, M., and Ashjian, P. (2002). Human adipose tissue is a source of multipotent stem cells. Molecular biology of the cell *13*, 4279-4295. 10.1091/mbc.E02.
39. Sengenès, C., Miranville, A., Maumus, M., de Barros, S., Busse, R., and Bouloumié, A. (2007). Chemotaxis and differentiation of human adipose tissue CD34+/CD31- progenitor cells: role of stromal derived factor-1 released by adipose tissue capillary endothelial cells. Stem cells (Dayton, Ohio) *25*, 2269-2276. 10.1634/stemcells.2007-0180.
40. Rondini, E.A., Ramseyer, V.D., Burl, R.B., Pique-Regi, R., and Granneman, J.G. (2021). Single cell functional genomics reveals plasticity of subcutaneous white adipose tissue (WAT) during early postnatal development. Molecular Metabolism *53*, 101307. https://doi.org/10.1016/j.molmet.2021.101307.
41. Lee, K.F., Li, E., Huber, L.J., Landis, S.C., Sharpe, A.H., Chao, M.V., and Jaenisch, R. (1992). Targeted mutation of the gene encoding the low affinity NGF receptor p75 leads to deficits in the peripheral sensory nervous system. Cell *69*, 737-749. 10.1016/0092-8674(92)90286-L.
42. Chao, M.V. (2003). Neurotrophins and their receptors: A convergence point for many signalling pathways. Nature Reviews Neuroscience *4*, 299-309. 10.1038/nrn1078.
43. Laplante, M., and Sabatini, David M. (2012). mTOR Signaling in Growth Control and Disease. Cell *149*, 274-293. 10.1016/j.cell.2012.03.017.
44. Chen, G., Chen, S.M., Wang, X., Ding, X.F., Ding, J., and Meng, L.H. (2012). Inhibition of chemokine (CXC motif) ligand 12/chemokine (CXC motif) receptor 4 axis (CXCL12/CXCR4)-mediated cell migration by targeting mammalian target of rapamycin (mTOR) pathway in human gastric carcinoma cells. J Biol Chem *287*, 12132-12141. 10.1074/jbc.M111.302299.
45. Vogeser, M., König, D., Frey, I., Predel, H.-G., Parhofer, K.G., and Berg, A. (2007). Fasting serum insulin and the homeostasis model of insulin resistance (HOMA-IR) in the monitoring of lifestyle interventions in obese persons. Clinical Biochemistry *40*, 964-968. https://doi.org/10.1016/j.clinbiochem.2007.05.009.
46. Shimizu, Y., Kondo, K., Hayashida, R., Sasaki, K.I., Ohtsuka, M., Fukumoto, Y., Takashima, S., Inoue, O., Usui, S., Takamura, M., et al. (2022). Therapeutic angiogenesis for patients with no-option critical limb ischemia by adipose-derived regenerative cells: TACT-ADRC multicenter trial. Angiogenesis.

10.1007/s10456-022-09844-7.

47. Gerhard-Herman, M.D., Gornik, H.L., Barrett, C., Barshes, N.R., Corriere, M.A., Drachman, D.E., Fleisher, L.A., Fowkes, F.G.R., Hamburg, N.M., Kinlay, S., et al. (2017). 2016 AHA/ACC Guideline on the Management of Patients With Lower Extremity Peripheral Artery Disease: Executive Summary: A Report of the American College of Cardiology/American Heart Association Task Force on Clinical Practice Guidelines. Circulation *135*, e686-e725. doi:10.1161/CIR.0000000000000470.

48. Bode, D., Cull, A.H., Rubio-Lara, J.A., and Kent, D.G. (2021). Exploiting Single-Cell Tools in Gene and Cell Therapy. Frontiers in Immunology *12*. 10.3389/fimmu.2021.702636.

49. Hashmi, S., Ahmed, M., Murad, M.H., Litzow, M.R., Adams, R.H., Ball, L.M., Prasad, V.K., Kebriaei, P., and Ringden, O. (2016). Survival after mesenchymal stromal cell therapy in steroid-refractory acute graft-versus-host disease: systematic review and meta-analysis. The Lancet Haematology *3*, e45-e52. https://doi.org/10.1016/S2352-3026(15)00224-0.

50. Kelly, K., and Rasko, J.E.J. (2021). Mesenchymal Stromal Cells for the Treatment of Graft Versus Host Disease. Frontiers in Immunology *12*. 10.3389/fimmu.2021.761616.

51. Smith, R.J.P., Faroni, A., Barrow, J.R., Soul, J., and Reid, A.J. (2021). The angiogenic potential of CD271+ human adipose tissue-derived mesenchymal stem cells. Stem Cell Research & Therapy *12*, 160. 10.1186/s13287-021-02177-0.

52. Kohli, N., Al-Delfi, I.R.T., Snow, M., Sakamoto, T., Miyazaki, T., Nakajima, H., Uchida, K., and Johnson, W.E.B. (2019). CD271-selected mesenchymal stem cells from adipose tissue enhance cartilage repair and are less angiogenic than plastic adherent mesenchymal stem cells. Scientific Reports *9*, 3194. 10.1038/s41598-019-39715-z.

53. Méndez-Maldonado, K., Vega-López, G.A., Aybar, M.J., and Velasco, I. (2020). Neurogenesis From Neural Crest Cells: Molecular Mechanisms in the Formation of Cranial Nerves and Ganglia. Frontiers in Cell and Developmental Biology *8*. 10.3389/fcell.2020.00635.

54. Um, S.H., Frigerio, F., Watanabe, M., Picard, F., Joaquin, M., Sticker, M., Fumagalli, S., Allegrini, P.R., Kozma, S.C., Auwerx, J., and Thomas, G. (2004). Absence of S6K1 protects against age- and diet-induced obesity while enhancing insulin sensitivity. Nature *431*, 200-205. 10.1038/nature02866.

55. Rupnick, M.A., Panigrahy, D., Zhang, C.Y., Dallabrida, S.M., Lowell, B.B., Langer, R., and Folkman, M.J. (2002). Adipose tissue mass can be regulated through the vasculature. Proceedings of the National Academy of Sciences *99*, 10730-10735. 10.1073/pnas.162349799.

56. Xu, H., Barnes, G.T., Yang, Q., Tan, G., Yang, D., Chou, C.J., Sole, J., Nichols, A., Ross, J.S., Tartaglia, L.a., and Others (2003). Chronic inflammation in fat plays a crucial role in the development of obesity-related insulin resistance. Journal of Clinical Investigation *112*, 1821-1830. 10.1172/JCI200319451.Introduction.

57. Goossens, G.H., Bizzarri, A., Venteclef, N., Essers, Y., Cleutjens, J.P., Konings, E., Jocken, J.W.E., Čajlaković, M., Ribitsch, V., Clément, K., and Blaak, E.E. (2011). Increased adipose tissue oxygen tension

in obese compared with lean men is accompanied by insulin resistance, impaired adipose tissue capillarization, and inflammation. Circulation *124*, 67-76. 10.1161/CIRCULATIONAHA.111.027813.

58. Crewe, C., An, Y.A., and Scherer, P.E. (2017). The ominous triad of adipose tissue dysfunction: Inflammation, fibrosis, and impaired angiogenesis. Journal of Clinical Investigation *127*, 74-82. 10.1172/JCI88883.
59. Gimble, J.M., Bunnell, B.A., Chiu, E.S., and Guilak, F. (2011). Concise Review: Adipose-Derived Stromal Vascular Fraction Cells and Stem Cells: Let's Not Get Lost in Translation. Stem Cells *29*, 749-754. 10.1002/stem.629.
60. Varghese, J., Griffin, M., Mosahebi, A., and Butler, P. (2017). Systematic review of patient factors affecting adipose stem cell viability and function: implications for regenerative therapy. Stem Cell Research & Therapy *8*, 45-45. 10.1186/s13287-017-0483-8.
61. Rennert, R.C., Sorkin, M., Januszyk, M., Duscher, D., Kosaraju, R., Chung, M.T., Lennon, J., Radiya-Dixit, A., Raghvendra, S., Maan, Z.N., et al. (2014). Diabetes impairs the angiogenic potential of adipose-derived stem cells by selectively depleting cellular subpopulations. Stem Cell Research & Therapy *5*, 1-12. 10.1186/scrt468.
62. Inoue, O., Usui, S., Takashima, S.I., Nomura, A., Yamaguchi, K., Takeda, Y., Goten, C., Hamaoka, T., Ootsuji, H., Murai, H., et al. (2019). Diabetes impairs the angiogenic capacity of human adipose-derived stem cells by reducing the CD271(+) subpopulation in adipose tissue. Biochem Biophys Res Commun *517*, 369-375. 10.1016/j.bbrc.2019.07.081.
63. Stoeckius, M., Hafemeister, C., Stephenson, W., Houck-Loomis, B., Chattopadhyay, P.K., Swerdlow, H., Satija, R., and Smibert, P. (2017). Simultaneous epitope and transcriptome measurement in single cells. Nature Methods *14*, 865-868. 10.1038/nmeth.4380.
64. Katagiri, T., Kondo, K., Shibata, R., Hayashida, R., Shintani, S., Yamaguchi, S., Shimizu, Y., Unno, K., Kikuchi, R., Kodama, A., et al. (2020). Therapeutic angiogenesis using autologous adipose-derived regenerative cells in patients with critical limb ischaemia in Japan: a clinical pilot study. Scientific Reports *10*, 1-12. 10.1038/s41598-020-73096-y.
65. Vijay, J., Gauthier, M.F., Biswell, R.L., Louiselle, D.A., Johnston, J.J., Cheung, W.A., Belden, B., Pramatarova, A., Biertho, L., Gibson, M., et al. (2020). Single-cell analysis of human adipose tissue identifies depot and disease specific cell types. Nat Metab *2*, 97-109. 10.1038/s42255-019-0152-6.
66. Rondini, E.A., Ramseyer, V.D., Burl, R.B., Pique-Regi, R., and Granneman, J.G. (2021). Single cell functional genomics reveals plasticity of subcutaneous white adipose tissue (WAT) during early postnatal development. Mol Metab *53*, 101307. 10.1016/j.molmet.2021.101307.
67. Ganan-Gomez, I., Yang, H., Ma, F., Montalban-Bravo, G., Thongon, N., Marchica, V., Richard-Carpentier, G., Chien, K., Manyam, G., Wang, F., et al. (2022). Stem cell architecture drives myelodysplastic syndrome progression and predicts response to venetoclax-based therapy. Nat Med *28*, 557-567. 10.1038/s41591-022-01696-4.

68. Moison, C., Spinella, J.-F., Chagraoui, J., Lavallée, V.-P., Lehnertz, B., Thiollier, C., Boivin, I., Mayotte, N., MacRae, T., Marinier, A., et al. (2022). HMGA2 expression defines a subset of human AML with immature transcriptional signature and vulnerability to G2/M inhibition. Blood Advances *6*, 4793-4806. https://doi.org/10.1182/bloodadvances.2021005828.

69. Korsunsky, I., Millard, N., Fan, J., Slowikowski, K., Zhang, F., Wei, K., Baglaenko, Y., Brenner, M., Loh, P.r., and Raychaudhuri, S. (2019). Fast, sensitive and accurate integration of single-cell data with Harmony. Nature Methods *16*, 1289-1296. 10.1038/s41592-019-0619-0.

70. Vuong, H., Truong, T., Phan, T., and Pham, S. (2020). Venice: A New Algorithm for Finding Marker Genes in Single-Cell Transcriptomic Data. bioRxiv, 2020.2011.2016.384479. 10.1101/2020.11.16.384479.

71. Consortium, G.O. (2004). The Gene Ontology (GO) database and informatics resource. Nucleic Acids Research *32*, D258-D261. 10.1093/nar/gkh036.

72. Le, T., Phan, T., Pham, M., Tran, D., Lam, L., Nguyen, T., Truong, T., Vuong, H., Luu, T., Phung, N., et al. (2020). BBrowser: Making single-cell data easily accessible. bioRxiv, 2020.2012.2011.414136-412020.414112.414111.414136. 10.1101/2020.12.11.414136.